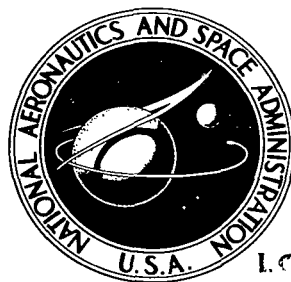


NASA TECHNICAL NOTE



NASA TN D-8426 *c.1*

NASA TN D-8426

LOAN COPY: RE  
AFWL TECHNICAL  
KIRTLAND AFB



THE EFFECT OF FORWARD SPEED  
ON J85 ENGINE NOISE FROM  
SUPPRESSOR NOZZLES AS  
MEASURED IN THE NASA-AMES  
40- BY 80-FOOT WIND TUNNEL

*Adolph Atencio, Jr.*

*Ames Research Center*

*and U.S. Army Air Mobility R&D Laboratory*

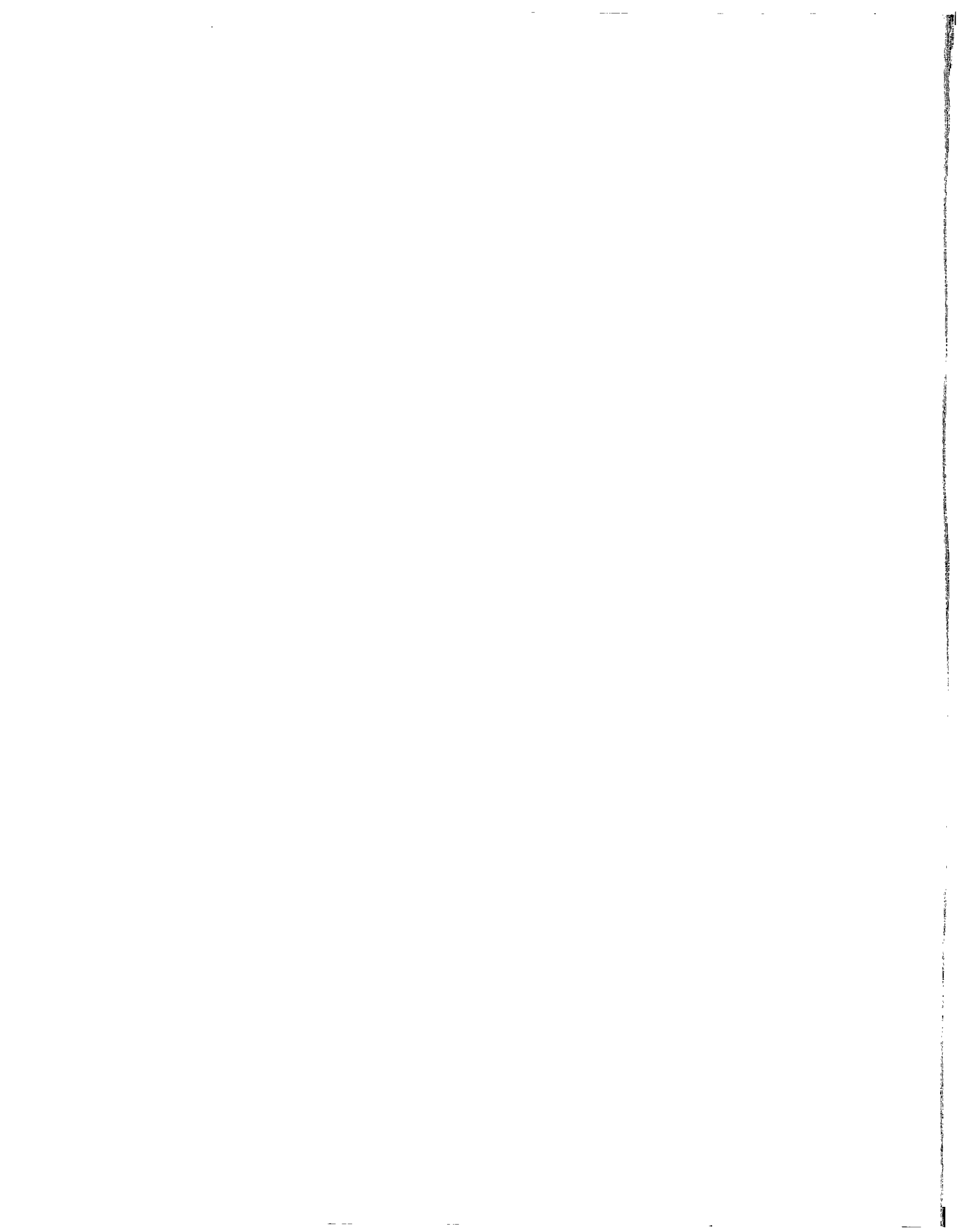
*Moffett Field, Calif. 94035*





0134196

1. Report No. NASA TN D-8426	2. Government Accession No.	3. Recipient's Catalog No.	
4. Title and Subtitle THE EFFECT OF FORWARD SPEED ON J85 ENGINE NOISE FROM SUPPRESSOR NOZZLES AS MEASURED IN THE NASA-AMES 40- BY 80-FOOT WIND TUNNEL	5. Report Date February 1977		6. Performing Organization Code
	7. Author(s) Adolph Atencio, Jr.		8. Performing Organization Report No. A-6592
9. Performing Organization Name and Address Ames Research Center and Ames Directorate U.S. Army Air Mobility R&D Laboratory	10. Work Unit No. 743-03-11		11. Contract or Grant No.
	12. Sponsoring Agency Name and Address National Aeronautics and Space Administration Washington, D.C. 20546		13. Type of Report and Period Covered Technical Note
15. Supplementary Notes		14. Sponsoring Agency Code	
16. Abstract <p>An investigation to determine the effect of forward speed on the exhaust noise from a conical ejector nozzle and three suppressor nozzles mounted behind a J85 engine was performed in the Ames 40-by 80-Foot Wind Tunnel. The nozzles were tested at three engine power settings and at wind-tunnel forward speeds up to 91 m/sec (300 ft/sec). In addition, outdoor static tests were conducted at the Ames Outdoor Static Test Facility to determine (1) the differences between near-field and far-field measurements, (2) the effect of an airframe on the far-field directivity of each nozzle, and (3) the relative suppression of each nozzle with respect to the baseline conical ejector nozzle. It was found that corrections to near-field data are necessary to extrapolate to far-field data and that the presence of the airframe changed the far-field directivity as measured statically. The results show that the effect of forward speed was to reduce the noise from each nozzle more in the area of peak noise, but the change in forward quadrant noise was small or negligible. A comparison of wind-tunnel data with available flight-test data shows good agreement.</p>			
17. Key Words (Suggested by Author(s)) Aircraft noise Jet noise Wind-tunnel noise measurement		18. Distribution Statement Unlimited  STAR Category - 07	
19. Security Classif. (of this report) Unclassified	20. Security Classif. (of this page) Unclassified	21. No. of Pages 65	22. Price* \$4.25



## NOMENCLATURE

$A_{E_8}$	effective nozzle area, $m^2$ ( $ft^2$ )
$c_o$	speed of sound, $m/sec$ ( $ft/sec$ )
$FF$	far field
$NF$	near field
$OASPL$	overall sound pressure level, $dB$ re $20$ dynes/ $cm^2$
$PNL$	perceived noise level, $PNdB$
$P_o$	ambient pressure, $N/m^2$ ( $lb/ft^2$ )
$P_8$	exhaust nozzle total pressure, $N/m^2$ ( $lb/ft^2$ )
$R$	ray distance from nozzle exit plane centerline to microphone, $m$ ( $ft$ )
$SPL$	sound pressure level, $dB$ re $20$ dynes/ $cm^2$
$T_o$	ambient temperature, $^{\circ}K$ , $^{\circ}R$
$T_8$	jet exhaust total temperature, $^{\circ}K$ , $^{\circ}R$
$V_j, V_8$	jet exit velocity, $m/sec$ ( $ft/sec$ )
$V_o$	wind-tunnel (flight) velocity, $m/sec$ ( $ft/sec$ )
$V_R$	relative velocity ( $V_j - V_o$ or $V_8 - V_o$ ), $m/sec$ ( $ft/sec$ )
$W_8$	total weight flow of engine
$\theta_I$	acoustic angle referenced to engine inlet axis, $deg$

**THE EFFECT OF FORWARD SPEED ON J85 ENGINE NOISE FROM  
SUPPRESSOR NOZZLES AS MEASURED IN THE NASA-AMES  
40- BY 80-FOOT WIND TUNNEL**

Adolph Atencio, Jr.

Ames Research Center  
and  
Ames Directorate  
U. S. Army Air Mobility R&D Laboratory

**SUMMARY**

An investigation to determine the effect of forward speed on the exhaust noise from a conical ejector nozzle and three suppressor nozzles mounted behind a J85 engine was performed in the Ames 40- by 80-Foot Wind Tunnel. The nozzles were tested at three engine power settings and at wind-tunnel forward speeds up to 91 m/sec (300 ft/sec). In addition, outdoor static tests were conducted at the Ames Outdoor Static Test Facility to determine (1) the differences between near-field and far-field measurements, (2) the effect of an airframe on the far-field directivity of each nozzle, and (3) the relative suppression of each nozzle with respect to the baseline conical ejector nozzle. It was found that corrections to near-field data are necessary to extrapolate to far-field data and that the presence of the airframe changed the far-field directivity as measured statically. The results show that the effect of forward speed was to reduce the noise from each nozzle more in the area of peak noise, but the change in forward quadrant noise was small or negligible. A comparison of wind-tunnel data with available flight-test data shows good agreement.

**INTRODUCTION**

The staff at Ames Research Center has been using the 40- by 80-foot wind tunnel to determine the effect of forward speed on various aircraft noise sources such as propellers, lift fans, and jet engines. Comparisons of wind-tunnel data with available flight-test data have shown good agreement (refs. 1 and 2). The use of a large-scale wind tunnel where actual engines and boiler plate suppressor hardware can be tested will substantially reduce the cost of determining acoustic characteristics of configurations.

An experimental study to determine the effect of forward speed on the noise from a conical ejector nozzle (baseline) and three suppressor nozzles on a J85-5 turbojet engine was performed in the 40- by 80-foot wind tunnel. The nozzles were flight-test hardware from a Lewis Research Center F106B flight-test program (ref. 3). The nozzles were mounted in a nacelle that was tested both in an isolated installation and then under the right wing of an aircraft research model. Tests were initially performed at the Ames Static Test Facility to determine the relationship of data measured near the nacelle (such as wind-tunnel measurements) to data measured in the far-field to

determine the effect of an airframe on the far-field directivity for each nozzle and to determine the relative suppression of each nozzle with respect to the conical ejector nozzle. The wind-tunnel tests were performed to determine the effect of forward speed on the noise from each nozzle. The wind-tunnel data were also compared with flight-test data to verify the wind-tunnel results. All four nozzles were tested in both model configurations except during the wind-tunnel tests, where only the conical ejector nozzle and the auxiliary inlet ejector nozzles were tested in the isolated nacelle configuration. The data presented here have been corrected to free field except for the static data comparisons from more than one source.

## MODEL DESCRIPTION

### Nozzles

The nozzles tested were the conical ejector nozzle, an auxiliary inlet ejector nozzle (AIE), a 32-spoke nozzle (32 spoke), and a 104 elliptical tube mixer suppressor nozzle (104 tube) with an acoustically treated ejector shroud (figs. 1-4). The nozzles were mounted in a nacelle with a General Electric J85-5 turbojet engine. The nacelle was tested in an isolated installation and then under the right wing of an aircraft research model. A bellmouth inlet was used for static tests and a sharp lip inlet was used for the forward speed tests in the wind tunnel. The conical ejector nozzle and AIE nozzle installation used a standard afterburner (A/B) with variable exit nozzle, but the 104-tube nozzle and 32-spoke nozzle required a modified fixed nozzle area A/B. Both versions of the A/B are shown in figure 5. The inlet included an annular ring bypass valve that was run fully closed during most of the tests. A summary description of each nozzle follows.

*Conical ejector nozzle*— The conical ejector nozzle (fig. 1) consists of a conical convergent primary nozzle with a cylindrical secondary ejector. The ejector was designed to pump 4 to 6 percent of the primary flow for cooling purposes.

*AIE nozzle*— The auxiliary inlet ejector nozzle is shown in figure 2. The nozzle incorporates a series of 16 auxiliary inlet doors located around the periphery of the external skin ahead of the primary nozzle. The principal purpose of the doors is to allow outside air to enter the ejector and provide an aerodynamically smaller ejector exit area that helps reduce the over expansion of the primary jet at low values of nozzle pressure ratio. Additional details may be found in reference 4.

*32-Spoke area ratio nozzle*— The 32-spoke nozzle (fig. 3) had an area ratio of 2.0, meaning the total annulus area divided by the flow area equals 2 or the blocked area is equal to the flow area. The blocker elements had a shallow "V" design with radially tapered sides and, therefore, each flow element is nearly rectangular in shape.

*104-Elliptical-tube mixer suppressor nozzle*— The 104-tube nozzle is shown in figure 4 with the acoustic shroud. The elliptical tubes, arranged in concentric rings, are mounted on a conical base plate with the major axis radial. All tubes of a given ring have the same length. The tubes of the outer ring are longest, 9.22 cm (3.63 in.). The ratio of the area that circumscribes the mixing nozzle to the primary effective area is 2.8. The ventilation factor (or the ratio of side-flow area between outer row of tubes to base area) is about 0.6. The acoustic shroud had a maximum cavity depth of 4.57 cm (1.81 in.), resulting in a shroud exit diameter of 53.80 cm (21.18 in.). The outer surface of

the shroud had a boattail angle of  $10^\circ$  and a boattail juncture radius of 0.5 nacelle diameters. The acoustic treatment consisted of a perforated plate adjacent to the jet, a bulk absorber, and a solid backing plate. Additional detail is given in reference 3.

### Aircraft Model

The aircraft model used for these tests was a 3/4-scale model of the F-15 aircraft. The engine was mounted under the right wing of the aircraft model, 2.1 m off the centerline to duplicate the F106B flight-test nozzle position with respect to the wing. Figure 6 is a schematic of the aircraft model. The installation included a specially designed flap for the AIE nozzle, which was also used when the other nozzles were tested. The flap is shown with the AIE nozzle in figure 7. Since the F-15 differs from the F106B aircraft, the reflecting surfaces were not identical to the F106B installation and therefore the wind-tunnel installation was a compromise to simulate as nearly as possible the F106B nozzle installations.

## HARDWARE INSTALLATION

The flight nacelle with the test nozzles was mounted both in an isolated configuration and under the right wing of the F-15 aircraft research model. The installation for the isolated configuration and for the under-the-wing position for both the outdoor static testing and for the wind-tunnel tests was with the engine center line 6.1 m (20 ft) off the ground plane surface. Figures 8 and 9 show the outdoor static test installation and figures 10 and 11 show the wind-tunnel installation.

During static testing and for the zero forward speed runs in the wind tunnel, the bottom half of the nacelle was removed and the bellmouth inlet was used. The wind-tunnel forward speed tests were performed with the bottom half of the nacelle in place and with a sharp lip flight inlet. Cooling air was supplied to the engine during the static tests outdoors by a portable compressor located approximately 25 m (75 ft) from the engine centerline on the left-hand side of the model. In the wind tunnel, cooling air was provided from the plant air source. In both cases, the engine exhaust noise was 10 dB or more above the cooling air noise for all test conditions and configurations.

## INSTRUMENTATION

### Nozzle and Engine

The instrumentation on the engine and nozzles was used to determine nozzle exit jet velocity. The instrumentation measured engine inlet total pressures, compressor face total pressure and temperature, turbine exit total pressure and temperatures, fuel flow, compressor rpm, and nozzle exit area. The exit jet velocity was determined by inputting the various parameters to a propulsion program supplied by Lewis Research Center.

## Acoustic

The microphones were 1.27-cm (0.5-in.) B&K 4133 condenser type microphones with B&K 2619 cathode followers. The microphone system was connected by lengths of cable to B&K power supplies, and the output from the power supplies were connected to Ampex FR 1300A tape recorders. The tape recorders had a center frequency of 54 kHz and were run at 30 ips. Data were recorded on 12 FM channels with time code and voice recorded. The cathode followers, cables, and power supplies were calibrated with a random pink noise generator before each series of tests. Before each run, the microphone systems were calibrated with a piston phone producing a 124-dB signal at 250 Hz.

Microphones for static testing were set up to duplicate the wind-tunnel installation and were also set on a 30.5-m (100-ft) radius arc with respect to the nozzle exit plane centerline. The microphones set up to duplicate the wind-tunnel position were 1.83 m (6 ft) off the concrete surface, while the microphones on the 30.5-m-radius arc were 6.1 m (20 ft) above the concrete surface at engine centerline height. Figures 12 and 13 are schematics of the wind-tunnel microphone positions and figure 14 shows the microphones on the 30.5-m arc. For static tests, bulb wind screens were used on the far-field microphones and bullet nose wind screens were used on the near-field microphones. With the wind screens in place, the microphones were omnidirectional within  $\pm 1.5$  dB. The bullet nose wind screens were used on all microphones during the wind-tunnel tests.

## TEST PROCEDURE

For the static outdoor tests, a predetermined engine exhaust pressure was set, and propulsion data and acoustic data were recorded simultaneously, with approximately 2 min of acoustic data recording. The wind-tunnel test procedure was essentially the same except that the wind-tunnel forward speed was held constant while the engine power was varied to give a range of relative velocities. Four tunnel forward speeds and three exhaust pressures were used during the wind-tunnel tests. A summary of test conditions is given in table I. The static outdoor tests were run during early morning hours to minimize background noise and to avoid wind conditions above 5 knots wind velocity.

## DATA REDUCTION AND ANALYSIS

### Data Reduction

The data from engine and nozzle instrumentation were fed into a propulsion program supplied by Lewis Research Center. Calculations were made to determine jet exit velocity, wind-tunnel velocity, relative velocity, engine pressure ratio, corrected engine rpm, and various condition-monitoring parameters.

The acoustic data were reduced to digital form using a 1/3-octave analyzer and then inputting the digitized data to a computer program. The output of the computer program was 1/3-octave

spectrum listings of *SPL* versus 1/3-octave center frequency, *OASPL*, *PNL*, and sound power level for selected conditions. The data were corrected for background noise where possible before final output. The data reduction procedure is summarized in reference 6; reference 6 also includes summary tables of engine conditions, wind-tunnel velocities, and plots of the reduced acoustic data versus combinations of wind-tunnel velocity and engine conditions for the various microphone positions. The static outdoor measurements are summarized in a similar manner. The repeatability of data as a check on data accuracy is within  $\pm 2$  dB.

## Corrections

*Reverberations*— Data from the outdoor static tests were used to establish free-field data for the wind-tunnel microphone positions. The outdoor free-field data were assembled by correcting the measured data for ground reflections using the method of reference 7. This method assumes the source to emit stationary random noise which satisfies the ergodic hypothesis, that the receiver is in the acoustic far field, that the atmosphere in which the source propagates is isothermic, immobile, and homogeneous, and that the surface above which measurements are made is smooth, and that the reflections are specular. Due to wavelength considerations and source dimension, the corrections are believed accurate down to 160 Hz for this test. The free-field data from the static test were compared with wind-tunnel data at the same conditions (zero tunnel speed). The incremental differences in *SPL* at each 1/3-octave center frequency were then used to correct wind-tunnel data for the reverberant field. The procedure was followed for each nozzle and for each power setting to establish corrections for all test conditions with the tunnel off. A summary of the corrections is given in tables II and III for the isolated nacelle and under wing configurations, respectively.

*Emission angle*— To make valid comparisons of the wind-tunnel data with flight-test data, the wind-tunnel data were corrected for convection of sound waves in the wind tunnel. Adjusting the data to a comparable emission angle was done by use of geometrical considerations for correct microphone positions. The change in microphone position was determined using a simple transformation involving wind-tunnel velocity ( $V_o$ ), speed of sound ( $c_o$ ), and the ray distance ( $R$ ) of the fixed microphone back to the referenced source location at the nozzle exit plane. The change in microphone position parallel to the wind-tunnel centerline was equal to  $RV_o/c_o$ . The flight data were corrected to the angle at time of noise emission by use of retarded time to reduce proper data.

*Doppler shift and atmospheric attenuation*— The comparison of wind-tunnel data with flight data requires that the data be at the same distance with ground reflection (ref. 7) and Doppler effects removed. The data from the wind tunnel were not corrected for the Doppler shift since the microphone and model had no relative motion between them. The wind-tunnel data were corrected to the flight distances, however, and atmospheric attenuation was accounted for by use of reference 8. The data for comparison with flight results were corrected to a standard day condition of 70° F and 77 percent relative humidity. The flight data were corrected to free field and standard day and for Doppler shift by Lewis Research Center. The wind-tunnel data in reference 6 are corrected to a standard day of 59° F and 70 percent relative humidity.

## RESULTS AND DISCUSSION

### Outdoor Static Tests

Data from the outdoor static tests were plotted to show the far-field directivity for each nozzle as compared to the baseline conical ejector nozzle. Figure 15 shows data for an exit velocity of 594 m/sec (1950 ft/sec) for the 30.5-m-radius arc and isolated nacelle configuration. The peak noise angle is different for the various nozzles tested. The figure shows that the conical nozzle noise, the 32-spoke nozzle noise, and the AIE nozzle noise peak at  $130^\circ$ . The 104-tube nozzle without shroud noise peaks at  $120^\circ$  while the 104-tube nozzle with shroud shows a peak noise at  $110^\circ$ . The suppression shown with respect to the peak noise angle for the conical nozzle is as follows: the 32-spoke nozzle shows 7-PNdB suppression, the AIE shows -1-PNdB suppression, the 104-tube nozzle with the shroud shows 17-PNdB suppression.

*Installation effect*— Figure 16 shows noise directivity data for the nacelle under wing configuration. Figure 17 shows data from both figures 15 and 16 for comparison. The differences in installation produced a directivity change. For the conical nozzle, there was an increase in forward quadrant noise of from 1 to 3 PNdB when the wing was added and a decrease of 1 to 2 PNdB for most of the aft quadrant noise. The 32-spoke nozzle shows a slight increase in noise in the forward quadrant and little or no change in the aft quadrant when the engine was mounted under the wing. The data for the 104-tube nozzle with the acoustic shroud show that forward quadrant noise increased 1 PNdB and that peak noise decreased by 2 to 3 PNdB. The effect of the model therefore was different for each nozzle and suggests that the installation effects can alter the observed effectiveness of suppressors. The general practice of testing isolated engines on test stands and comparing that data with an engine installed on an aircraft for flyover may result in erroneous conclusions. Table IV summarizes results from figures 15, 16, and 17.

Figures 18 through 20 compare data measured at the Ames Static Test Facility for the under wing installation with data measured in ground static tests at Lewis Research Center. The figures show data measured on a 30.5-m-radius arc for the conical ejector and 104-tube nozzles. The agreement is fair over all angles of measurements.

*Comparisons of near-field and far-field data*— Data from the Ames Static Test Facility were measured on 4.3-m (14-ft) and 5.4-m (18-ft) sidelines and on a 30.5-m (100-ft) radius arc. All data were corrected for ground reflections; the geometrically near-field sideline measurements were extrapolated to the 30.5-m arc for comparison. The directivity shifted from near-field to far-field sidelines with peak noise occurring at a higher angle for the near-field sideline. Figure 21 shows data for the conical ejector nozzle in the isolated configuration. For the conical ejector nozzle, there are differences of up to 3 PNdB for angles between  $60^\circ$  and  $130^\circ$ ; with the 4.3-m and 5.5-m near measurements below the far field 30.5-m-arc data, perfect agreement at the peak noise angle, and differences of up to 5 PNdB for angles from  $150^\circ$  to  $170^\circ$  but with the near measurements higher. Figure 22 shows similar data for the 104-tube nozzle without the acoustic shroud. These data show agreement within 2 PNdB for angles up to  $140^\circ$ , but for angles from  $150^\circ$  to  $170^\circ$  the data show significant differences, with the 4.3-m data being 12 PNdB above the 30.5-m-arc data at  $170^\circ$ . The 5.4-m data are below the 30.5-m data, with differences of only 2 to 3 PNdB for these same angles. The discrepancy here may be due to jet impingement at the  $160^\circ$  and  $170^\circ$  microphone positions for the 4.3-m data and the breakdown of ground reflection corrections for these low-frequency,

high-level noise measurements (ref. 6). The data from figures 21 and 22 show that noise measurements made in a geometrically near field should be corrected for directivity when extrapolated to far-field distances.

### Wind-Tunnel Tests

Noise measurements were made for various combinations of wind-tunnel forward speed and engine power settings. The engine power setting was varied while the tunnel speed was held constant. A range of relative velocities was established for each nozzle to determine the effect of forward speed on noise. The measurements obtained at each microphone position are similar to the 1/3-octave spectrums shown in figure 23.

*Peak noise*— The effect of forward speed on peak noise is shown for the conical ejector nozzle in figure 24 for the nacelle mounted under the wing. The figure shows that as wind-tunnel forward speed is increased at constant engine power setting, the noise is reduced. The peak noise for the conical nozzle follows a relative velocity relationship where the change in *OASPL* can be directly related to the change in relative velocity over the range of velocities tested.

Figure 25 shows similar data for the 104-tube nozzle without the acoustic shroud. These data show that there is an additional effect of forward speed on peak noise than was shown for the conical nozzle. The forward speed increased the suppression of the noise relative to static, but the noise followed a relative velocity effect as power was reduced with tunnel speed held constant.

Figure 26 shows data for the 104-tube nozzle with the acoustic shroud. The addition of the shroud reduced *OASPL* by 4 dB for zero forward speed. The effect of increasing forward speed with the shroud shows no additional effect at 52 m/sec where results are similar to the conical ejector nozzle; at 91 m/sec, however, the data show increased reduction in *OASPL* as was shown for the 104-tube nozzle without the acoustic shroud.

Data for the 32-spoke nozzle and AIE nozzle are shown in figures 27 and 28, respectively. Peak noise from the 32-spoke nozzle followed a relative velocity change, but the change in level was not completely linear. The AIE peak noise change with relative velocity is somewhat similar to that shown for the 104-tube nozzle.

*Effect of forward velocity on directivity*— Data are shown in figures 29 through 33 for each nozzle tested. The data have been extrapolated to a 30.5-m (100-ft) sideline and corrected for convection and the geometric near field so that the forward speed effect shown is representative of flight effect.<sup>1</sup> Figure 29 shows data for the conical ejector nozzle. There is a change in *OASPL* with increasing forward speed, but the change in level is not consistent with angle. For angles near peak noise, there is a large reduction in noise with forward speed, but for angles smaller than 130°, there is no significant change in level. The effect of forward speed for the 104-tube nozzle with and without shroud and for the 32-spoke nozzle (figs. 31–33) is similar except little or no change is shown for angles less than 100°.

<sup>1</sup> Background noise problems limited the amount of useful data for the 104-tube nozzle and so the data shown are for a wind-tunnel forward speed of 52 m/sec (170 ft/sec) where all nozzles were free from background noise interference at the engine power setting shown.

Figure 30 shows data for the AIE nozzle. There is a reduction of 3.5 dB in peak noise and an almost constant change in level for angles less than 130°. The data at forward speed show about 2-dB reduction for the forward quadrant angles.

The effect of forward speed on noise in the forward quadrant as measured in the 40-by-80-foot wind tunnel has been observed in F106B flight tests (ref. 5), while reference 9 reports data from several aircraft where the forward quadrant noise from flight was shown to be higher than data measured statically for the same jet exit velocity. The reason for increased noise in the forward quadrant with flight is not yet understood, but possible causes have been suggested. Among suggested causes are internally generated engine noise that is not reduced with forward speed when exhausted through the jet tail pipe (ref. 10), dynamic effect due to relative motion between source and observer (ref. 9), flow-field interaction between engine exhaust and airframe installation, and, for some configurations, the presence of shock noise in the flow (ref. 11). Each of the suggested causes may contribute to the forward lift effect and each must be investigated further to determine its contribution, if any.

#### Comparison of Wind-Tunnel Data and Flyover Data

*Velocity index*— Flight data can be compared with wind-tunnel data by comparing the velocity index. The velocity index is determined from the following equation:

$$m = \frac{OASPL_{\text{static}} - OASPL_{\text{flight}}}{10 \log (V_j/V_R)}$$

where  $OASPL_{\text{static}}$  and  $OASPL_{\text{flight}}$  are measured data for the same emission angle and distance. The velocity index equation was developed by approximating Lighthill's equation for the intensity of jet noise based on the eighth power of jet velocity. The development of the index is given in reference 12. The velocity index was calculated for the 104-tube nozzle with and without the acoustic shroud. The flight-data velocity index was calculated using data supplied by Lewis Research Center; the wind-tunnel index was calculated using figures 31 and 32. The results are shown in figures 34 and 35 for the 104-tube nozzle without and with the shroud, respectively. The results for the 104-tube nozzle without the shroud show that the wind-tunnel velocity index is slightly less than the flight velocity index for angles up to 115°, and then the wind-tunnel index is slightly higher than the flight index for angles through 160°. The overall agreement is good. Figure 35 shows similar data for the 104-tube nozzle with the acoustic shroud. The data show excellent agreement through 150°. The data from figures 34 and 35 show that the wind-tunnel data adequately predict the flight effect on noise for these two nozzles. Note that the velocity index calculation is sensitive to changes in  $V_j/V_R$  and to the  $OASPL$  difference. For example, a 1.0-dB error in  $OASPL$  difference from figures 31 and 32 can result in an error of 2.0 in the value of the index  $m$ . A second method for comparing data from flight and from the wind tunnel is to extrapolate wind-tunnel measurement to flight measurement distances and compare absolute levels (this method is shown in the following section).

*Direct comparison with flight*— To verify the observations from the velocity index plots, comparisons were made of wind-tunnel data with the F106B flyover data for the conical ejector nozzle and for the 104 nozzle with and without the acoustic shroud. The data for the conical nozzle were obtained from reference 13. The flight data for the 104-tube nozzle comparison were obtained

from Lewis Research Center. The comparisons made are PNdB versus acoustic angle from the engine inlet axis where the flight data are from *PNL* time histories of the respective flights. The wind-tunnel data were corrected to flight distance, for reverberation, and for near-field/far-field differences before the comparisons were made. The flight data were corrected to standard day and for ground reflections and Doppler shift. Figure 36 shows data for the conical ejector nozzle. The data agree well within  $\pm 2$  dB over all angles shown. Figures 37 and 38 show the data for the 104-tube nozzle with and without the acoustic shroud, and again the data agree well at all angles. These plots confirm the observations of figures 34 and 35, which show that wind-tunnel data and flight data agree quite well.

A spectrum comparison is desirable to determine if flight data and wind-tunnel spectrums are identical. Figures 39 and 40 show data for the 104-tube nozzle where comparisons could be made within  $\pm 3^\circ$  of acoustic angle. The spectra in figure 39 for the 104-tube nozzle without the acoustic shroud agree within  $\pm 2$  dB at the nominal  $120^\circ$  position, while for the nominal  $140^\circ$  position, low frequencies and the high-frequency data are not in agreement. Figure 40 shows data for the 104-tube nozzle at nominal positions of  $121^\circ$  and  $109^\circ$ . The data for the  $121^\circ$  position are in good agreement over most of the spectra within  $\pm 3$  dB, while the data at the  $109^\circ$  position exhibit problems similar to that shown for the  $140^\circ$  position (fig. 39). The discrepancies at  $109^\circ$  (fig. 40) and  $140^\circ$  (fig. 39) are sometimes seen with near-field measurements, but they may also be due to ground reflections. These problems and their solution are discussed in detail in reference 14. For the overall sound pressure levels and perceived noise levels used here, a gross correction for near-field measurements was applied to these data.

## CONCLUSIONS

The data from wind-tunnel tests to determine the effect of forward speed agree with results observed in flight tests of these same nozzles. The wind-tunnel trends were an accurate reflection of trends observed with flight data. Actual comparisons with flight data show good agreement. Generally, this investigation has shown the following results:

1. Wind-tunnel data are an accurate reflection of flight data when the proper corrections and adjustments are made.
2. Flight effect is not consistent among the nozzles tested. In particular, the conical and 32-spoke nozzles showed a reduction in peak noise with increased forward speed that follows simple relative velocity, whereas the 104-tube and AIE nozzles showed greater suppression with forward speed than was predicted using simple relative velocity relationship, although the AIE nozzle was not as effective a suppressor as the 32-spoke or 104-tube nozzles. Forward quadrant noise is not reduced as much as aft quadrant noise. For the 104-tube and 32-spoke nozzles, it was shown that forward quadrant noise did not change with forward speed.
3. Static outdoor measurements showed that (a) the effect of a reflecting surface is to change the far-field directivity for noise from each nozzle and the change in directivity is different for each nozzle, and that (b) the comparison of near-field model measurements as required in the wind

tunnel to measurements made in the far field showed some differences in level and that directivity effects had to be accounted for when extrapolating the wind-tunnel data to the flight distance.

Ames Research Center

National Aeronautics and Space Administration

Moffett Field, Calif., 94035, August 20, 1976

#### REFERENCES

1. Atencio, Adolph, Jr.; and Soderman, P. T.: Comparison of Aircraft Noise Measured in Flight Test and in the NASA-Ames 40- by 80-Foot Wind Tunnel. AIAA Paper 73-1047, Oct. 1973.
2. Cook, Woodrow L; and Hickey, David H.: Correlation of Low-Speed Wind Tunnel and Flight Test Data for V/STOL Aircraft. NASA TM X-62,423, 1975.
3. Wilcox, Fred A.: Comparison of Ground and Flight Test Results Using a Modified F106B Aircraft. NASA TM X-71,439, 1973.
4. Burley, Richard R.: Flight Investigation of Airframe Installation Effects on an Auxiliary Inlet Ejector Nozzle on an Underwing Engine Nacelle. NASA TM X-2396, 1971.
5. Burley, Richard R.: Flight Velocity Effects on the Jet Noise of Several Variations of a 104-Tube Suppressor Nozzle. NASA TM X-3049, 1974.
6. Beulke, M. R.; Clapper, W. S.; McCann, E. O.; and Morozumi, H. M.: A Forward Speed Effects Study on Jet Noise From Several Suppressor Nozzles in the NASA-Ames 40- by 80-Foot Wind Tunnel. NASA CR-114,741, 1974.
7. Thomas, P.: Acoustic Interference by Reflection-Application to Sound Pressure Spectrum of Jets. Aircraft Engine Noise and Sonic Boom, AGARD Conference Proceedings No. 42, North Atlantic Treaty Organization, Paris, France, 1969, pp. 1-20.
8. Harris, C. M.: Absorption of Sound in Air Versus Humidity and Temperature. NASA CR-647, 1967.
9. Bushell, K. W.: Measurement and Prediction of Jet Noise in Flight. AIAA Paper 75-461, March 1975.
10. Stone, James R.: On the Effects of Flight on Jet Engine Exhaust Noise. NASA TM X-71,819, 1975.
11. von Glahn, U.; and Goodykoontz, J.: Installation and Airspeed Effects on Jet Shock-Associated Noise. NASA TM X-71,792, 1975.
12. Cocking, B. J.; and Bryce, W. D.: An Investigation of the Noise of Cold Air Jets Under Simulated Flight Conditions. Rept. R 334, National Gas Turbine Establishment, Pyestock, England, Sept. 1974.
13. Brausch, J. F.: Flight Velocity Influence on Jet Noise of Conical Ejector, Annular Plug and Segmented Suppressor Nozzles. NASA CR-120,961, 1972.
14. Strout, F. C.: Flight Effects on Noise Generated by the JT8D-17 Engine in a Quiet Nacelle and Conventional Nacelle as Measured in the NASA Ames 40- by 80-Foot Wind Tunnel. NASA CR-137,797, 1976.

TABLE I.— TEST POINT AND CYCLE DATA

(a) Isolated nacelle outdoor static test

Nozzle	Data point	$V_8$ , m/sec	$T_{T8}$ , °K	$W_8$ , kg/sec	$P_8/P_0$	$A_{E8}$ , m <sup>2</sup>	rpm	$T_{O}$ , °K	$V_{O}$ , m/sec	Data type
Conical ejector	403	211.8	633	13.58	1.133	0.07465	13940	288	0	FF
	404	327.7	708	17.39	1.313	.08750	14889	288	0	
	405	419.1	753	19.69	1.532	.08768	15659	288	0	
	406	481.6	843	20.39	1.661	.08882	16247	290	0	
	407	583.4	953	20.74	1.957	.08180	16593	289	0	
	502	215.2	657	13.98	1.132	.07837	13810	289	0	NF
	503	349.3	731	17.25	1.351	.08568	14891	290	0	
	504	403.9	753	19.53	1.484	.08973	15602	291	0	
	505	483.4	868	20.41	1.643	.09126	16311	290	0	
	506	580.6	970	20.59	1.918	.08360	16543	290	0	
508	556.9	972	20.72	1.811	.08916	16608	291	0		
AIE	703	310.0	673	13.91	1.291	.06966	14146	290	0	FF
	704	360.3	713	15.92	1.390	.07631	14487	290	0	
	705	403.0	733	17.31	1.498	0.7801	15034	291	0	
	706	503.8	833	19.84	1.763	.08124	16160	291	0	
	707	526.4	833	20.06	1.863	.07781	16474	291	0	
	602	315.5	668	13.98	1.306	.06908	14130	288	0	NF
	603	358.1	703	15.59	1.391	.07387	14460	288	0	
	604	398.4	733	17.56	1.484	.08004	15033	289	0	
	605	501.7	833	20.06	1.753	.08274	16161	289	0	
	606	580.0	953	20.04	1.940	.08004	16509	289	0	
32 Spoke	1502	269.8	751	11.96	1.187	.06876	11696	286	0	FF
	1503	409.4	786	14.81	1.474	.07037	14124	286	0	
	1504	465.1	804	17.01	1.643	.07342	14847	286	0	
	1505	527.3	861	18.91	1.828	.07596	15456	287	0	
	1506	608.4	972	20.52	2.053	.07824	16283	288	0	
	1507	594.1	951	17.68	2.013	.06801	16254	289	0	
	1602	269.4	735	11.91	1.192	.06752	11772	288	0	NF
	1603	402.0	761	14.77	1.472	.06913	14094	288	0	
	1604	462.4	792	16.96	1.646	.07245	14831	288	0	
	1605	527.9	863	19.09	1.827	.07685	15450	289	0	
1606	594.1	953	20.47	2.010	.07895	16315	289	0		

TABLE I.— Continued

(a) Concluded

Nozzle	Data point	$V_8$ , m/sec	$T_{T_8}$ , °K	$W_8$ , kg/sec	$P_8/P_0$	$A_{E_8}$ , m <sup>2</sup>	rpm	$T_{O_8}$ , °K	$V_{O_8}$ , m/sec	Data type	
104 Tube without shroud	1402	270.7	718	12.00	1.198	0.06657	12415	286	0	FF	
	1403	403.9	762	15.69	1.477	.07296	14380	286	0		
	1404	470.9	812	17.56	1.656	.07525	14992	286	0		
	1405	493.2	838	18.19	1.712	.07671	15157	286	0		
	1406	537.4	879	19.10	1.848	.07651	15474	287	0		
	1407	570.6	903	19.81	1.971	.07548	15765	287	0		
	1408	599.9	938	20.27	2.067	.07513	15972	288	0		
	1409	593.8	957	20.43	2.002	.07902	16085	288	0		
	1302	264.3	676	12.03	1.201	.06458	12433	285	0		NF
	1303	403.0	741	13.86	1.491	.06294	13358	285	0		
	1304	465.7	790	17.53	1.661	.07389	14978	285	0		
	1305	533.1	864	19.18	1.851	.07604	15462	285	0		
	1306	584.0	914	20.20	2.032	.07548	15881	285	0		
	1307	609.3	961	20.57	2.079	.07677	16198	286	0		
104 Tube with shroud	1002	261.5	684	12.17	1.194	.06624	12659	287	0	FF	
	1003	397.8	737	14.55	1.479	.06647	14395	288	0		
	1004	471.8	803	15.65	1.668	.06633	14970	288	0		
	1005	488.9	800	15.96	1.741	.06466	15126	288	0		
	1006	539.5	868	16.54	1.873	.06503	15436	288	0		
	1007	577.9	930	19.75	1.965	.07667	15687	289	0		
	1008	583.4	937	20.10	1.981	.07774	15925	289	0		
	1009	513.9	947	20.20	1.674	.09300	16031	289	0		
	1102	273.1	730	12.03	1.199	.06733	12565	290	0		NF
	1103	403.9	766	15.65	1.473	.07320	14378	290	0		
1104	466.3	816	17.94	1.635	.07811	15108	290	0			
1105	531.6	871	18.98	1.834	.07627	15405	291	0			
1106	610.2	969	20.10	2.068	.07575	15951	291	0			

TABLE I.— Continued

(b) Isolated nacelle wind-tunnel test

Nozzle	Data point	$V_8$ , m/sec	$T_{T8}$ , °K	$W_8$ , kg/sec	$P_8/P_O$	$A_{E8}$ , m <sup>2</sup>	rpm	$T_O$ , °K	$V_O$ , m/sec	Data type
Conical ejector	301	264.0	649	12.90	1.210	0.06707	13533	293	5.7	NF
	302	382.2	708	16.06	1.455	.07267	14494	293	5.6	
	303	446.5	743	17.51	1.642	.07206	15119	293	4.9	
	304	507.8	804	19.71	1.820	.07624	15724	294	6.2	
	305	597.7	925	20.43	2.079	.07449	16327	294	6.5	
	306	463.3	778	17.28	1.665	.07184	15048	296	6.3	
	307	465.7	783	17.20	1.669	.07161	15020	297	5.9	
	308	566.6	783	17.09	1.670	.07111	14992	298	5.9	
	401	233.2	633	12.67	1.164	.06863	13435	287	45.3	NF
	405	374.9	723	14.80	1.423	.07030	14367	289	45.7	
	409	423.4	763	17.80	1.537	.08057	15078	292	45.9	
	413	566.6	918	18.58	1.928	.07391	15484	294	45.8	
	501	575.5	923	19.04	1.964	.07460	16160	300	52.3	NF
	505	258.8	677	14.27	1.192	.07965	13310	304	75.3	
	509	405.1	749	15.01	1.491	.07066	14331	307	75.6	
	513	473.7	796	17.24	1.685	.07416	15071	309	75.6	
601	604.4	929	19.82	2.109	.07553	16179	299	100.6	NF	
605	600.8	928	18.79	2.090	.07243	15628	310	103.0		
609	580.0	921	17.14	1.991	.06912	14964	317	103.7		
613	445.6	798	14.74	1.579	.06956	14242	321	104.2		
617	367.9	770	12.33	1.374	.06566	13276	323	104.3		
621	584.9	930	17.71	2.002	.07142	15620	319	103.5		
AIE	701	327.1	738	12.67	1.296	.06588	13437	297	4.5	NF
	704	377.0	770	14.44	1.396	.07131	14334	297	4.5	
	705	416.4	788	16.32	1.494	.07624	15004	297	4.5	
	709	537.1	928	18.07	1.783	.07709	15724	299	4.5	
	710	535.8	930	18.60	1.775	.07978	16112	299	4.5	

TABLE I.- Continued

(b) Concluded

Nozzle	Data point	$V_8$ , m/sec	$T_{T_8}$ , °K	$W_8$ , kg/sec	$P_8/P_0$	$A_{E_8}$ , m <sup>2</sup>	rpm	$T_0$ , °K	$V_0$ , m/sec	Data type
AIE concluded	901	299	718	(a)	1.263	(a)	(a)	(a)	45.7	NF
	902	369	783	↓	1.389	↓	↓	↓	45.7	
	903	396	813	↓	1.452	↓	↓	↓	45.7	
	904	494	928	↓	1.666	↓	↓	↓	45.7	
	905	511	928	↓	1.729	↓	↓	↓	45.7	
	1001	303	708	(a)	1.277	(a)	(a)	(a)	76	NF
	1002	372	773	↓	1.401	↓	↓	↓	76	
	1003	403	813	↓	1.464	↓	↓	↓	76	
	1004	499	893	↓	1.716	↓	↓	↓	76	
	1005	518	923	↓	1.773	↓	↓	↓	76	
	1006	326	731	↓	1.318	↓	↓	↓	76	
	1101	327.7	676	13.20	1.331	0.06844	13520	289	99.7	NF
	1102	442.6	746	15.67	1.623	.07015	14366	293	100.6	
	1103	459.6	798	16.34	1.629	.07556	15069	296	101.2	
	1104	516.3	928	17.50	1.701	.08391	15765	299	101.2	
	1105	494.4	928	17.78	1.623	.08941	15867	301	102.1	
1113	--	--	--	--	--	--	310	104		
1114	--	--	--	--	--	--	288	76		
1115	--	--	--	--	--	--	310	45.7		
1116	--	--	--	--	--	--	288	0		

<sup>a</sup>Data not available.

TABLE I.— Continued

(c) Wing nacelle outdoor static test

Nozzle	Data point	$V_8$ , m/sec	$T_{T_8}$ , °K	$W_8$ , kg/sec	$P_8/P_O$	$A_{E_8}$ , m <sup>2</sup>	rpm	$T_O$ , °K	$V_O$ , m/sec	Data type
32 Spoke	102	350.5	776	12.85	1.329	0.06709	13366	288	0	FF
	103	428.9	814	15.87	1.511	.07473	14435	287	0	
	104	527.0	873	19.36	1.810	.07899	15508	288	0	
	105	554.4	898	19.16	1.899	.07915	15812	288	0	
	106	606.6	972	20.63	2.045	.07876	16324	288	0	
	202	352.7	770	12.71	1.337	.06566	13318	291	0	NF
	203	432.2	812	15.43	1.523	.07189	14333	291	0	
	204	533.4	868	18.92	1.845	.07544	15403	292	0	
	205	562.7	898	19.67	1.940	.07592	15709	292	0	
	206	616.0	989	20.30	2.064	.07749	16212	293	0	
104 Tube with shroud	302	393.8	771	15.77	1.441	.07577	14479	287	0	FF
	303	459.3	823	17.37	1.602	.07777	15018	287	0	
	304	530.7	883	18.93	1.813	.07766	15518	287	0	
	305	551.7	908	19.27	1.874	.07763	15637	287	0	
	306	612.0	976	20.03	2.068	.07597	16150	288	0	
	402	371.3	738	15.71	1.402	.07584	14459	287	0	NF
	403	438.9	793	17.22	1.561	.07755	14984	287	0	
	404	514.2	868	18.84	1.762	.07882	15471	288	0	
	405	533.4	883	19.15	1.824	.07807	15589	289	0	
	406	585.2	953	20.01	1.965	.07884	16114	289	0	

TABLE I.— Continued

(c) Concluded

Nozzle	Data point	$V_8$ , m/sec	$TT_8$ , °K	$W_8$ , kg/sec	$P_8/P_0$	$AE_8$ , m <sup>2</sup>	rpm	$T_0$ , °K	$V_0$ , m/sec	Data type
104 Tube without shroud	602	400.5	771	15.50	1.460	0.07345	14410	289	0	FF
	603	459.0	807	17.08	1.617	.07484	14934	289	0	
	604	534.9	891	18.82	1.821	.07711	15475	290	0	
	605	555.7	908	19.10	1.891	.07615	15623	290	0	
	606	615.4	990	19.89	2.060	.07618	16041	291	0	
	502	397.5	764	15.25	1.457	.07207	14306	290	0	
	503	457.5	809	16.80	1.610	.07405	14824	291	0	
	504	534.9	886	18.46	1.827	.07516	15371	292	0	
	505	554.4	903	19.06	1.892	.07575	15567	292	0	
	506	616.6	983	19.78	2.079	.07477	16059	292	0	
Conical ejector	1202	588.0	966	20.63	1.960	.08162	16923	287	0	FF
	1203	563.9	923	20.33	1.908	.08073	16375	288	0	
	1204	501.7	851	20.25	1.731	.08488	16259	287	0	
	1205	507.5	858	20.24	1.746	.08448	16232	287	0	
	1206	387.1	734	17.84	1.450	.08253	15144	288	0	
	1207	306.6	681	14.99	1.280	.07556	14193	288	0	
	1208	595.6	963	20.49	2.000	.07928	16579	289	0	NF
	1302	603.2	981	20.25	2.012	.07860	16483	290	0	
	1303	567.2	934	19.97	1.908	.07971	16049	291	0	
	1304	510.2	865	20.08	1.749	.08394	16197	291	0	
1305	390.5	846	17.35	1.456	.08019	15001	290	0		
1306	315.8	698	14.38	1.292	.07269	14001	291	0		

TABLE I.— Continued

(d) Wing nacelle wind-tunnel test

Nozzle	Data point	$V_8$ , m/sec	$T_{T_8}$ , °K	$W_8$ , kg/sec	$P_8/P_0$	$A_{E_8}$ , m <sup>2</sup>	rpm	$T_0$ , °K	$V_0$ , m/sec	Data type	
Conical ejector	201	582.2	951	19.36	1.954	0.0778	16106	293	51.5	NF	
	202	534.3	894	19.16	1.814	.0803	15951	294	51.5		
	203	410.6	778	16.94	1.484	.0807	15274	297	51.8		
	204	405.7	777	16.86	1.471	.0810	15280	297	51.8		
	301	601.4	953	19.90	2.048	.0788	16410	296	89.3	NF	
	302	523.3	862	19.53	1.808	.0831	15978	297	89.3		
	303	602.3	957	19.51	2.048	.0777	16174	303	92.6		
	304	534.3	877	18.60	1.836	.0789	15614	304	92.9		
	401	594.1	964	19.82	1.992	.0800	16401	297	76.5	NF	
	402	528.2	868	19.14	1.822	.0799	15832	301	76.8		
	403	413.6	777	17.11	1.494	.0801	15156	303	76.5		
	500	—	—	—	—	—	—	—	0	NF	
	501	605.3	970	20.96	2.041	.0796	16690	288	0		
	502	504.4	845	20.39	1.75	.0841	16118	291	0		
	503	394.4	742	17.57	1.465	.0809	15006	292	0		
	601	608.4	962	20.90	2.072	.0775	16544	291	0		NF
602	504.7	834	20.48	1.766	.0827	16097	291	0			
603	404.2	751	17.24	1.488	.0782	14916	294	0			
AIE	701	606.2	967	19.78	2.051	.0769	16146	298	76.2	NF	
	702	536.8	886	19.21	1.835	.0798	15731	300	76.2		
	703	427.9	883	16.53	1.529	.0775	15029	303	76.2		
	704	599.8	946	19.28	2.054	.0752	15773	305	92.7		
	705	545.3	890	18.59	1.87	.0771	15526	307	92.7		
	801	589.5	967	19.68	1.966	.0783	16415	298	50.9	NF	
	802	534.9	889	19.30	1.823	.0793	15859	294	50.9		
	803	429.8	801	16.67	1.525	.0775	15160	301	51.5		
	804	429.8	801	16.63	1.516	.0779	15160	301	51.2		
	104 Tube with shroud	901	618.7	981	20.24	2.096	.0754	16050	296	0	NF
		902	526.7	867	18.86	1.818	.0760	15424	292	0	
903		448.9	774	16.97	1.615	.0725	14890	299	0		

TABLE I.— Concluded

(d) Concluded

Nozzle	Data point	$V_8$ , m/sec	$T_{T_8}$ , °K	$W_8$ , kg/sec	$P_8/P_0$	$A_{E_8}$ , m <sup>2</sup>	rpm	$T_{O_8}$ , °K	$V_{O_8}$ , m/sec	Data type	
104 Tube with shroud	1001	588	946	19.22	1.992	0.0750	15867	294	50.9	NF	
	1002	541.9	894	18.11	1.849	.0740	15493	297	51.2		
	1003	469.7	838	16.51	1.624	.0743	15108	297	51.8		
	1004	593.4	941	19.68	2.027	.0750	15756	300	43.3		
	1005	538.3	885	18.30	1.845	.0743	15352	303	42.7		
	1006	469.7	828	16.61	1.634	.0735	14970	304	42.4		
	1007	577.3	891	19.00	2.029	.0715	15565	308	67.4		
	1008	552.6	897	17.42	1.892	.0722	15275	308	93.6		
	1009	485.9	840	15.91	1.681	.0717	14851	310	94.2		
104 Tube without shroud	1101	593.4	953	19.48	2.007	.0758	15992	292	50.6	NF	
	1102	537.9	896	18.20	1.827	.0754	15522	295	51.2		
	1103	465.4	837	16.53	1.61	.0749	15115	297	51.5		
	1104	603.2	953	19.40	2.059	.0750	15830	298	76.8		
	1105	541.9	886	17.96	1.859	.0740	15373	299	76.5		
	1106	471.5	832	16.31	1.637	.0739	14972	301	76.8		
	1107	596.8	939	18.97	2.049	.0744	15637	304	93.3		
	1108	549.9	881	17.61	1.905	.0718	15341	307	93.6		
	1109	474.6	832	15.83	1.648	.0724	14827	309	93.9		
32 Spoke	1201	617.8	953	20.72	2.14	.0720	16238	288	0	NF	
	1202	522.7	861	19.23	1.807	.0775	15493	288	0		
	1203	451.1	799	17.14	1.597	.0751	14898	291	0		
32 Spoke	1301	617.5	955	20.64	2.135	.0719	16530	291	0	NF	
	1302	530.9	868	18.86	1.834	.0757	15458	293	0		
	1303	431.9	802	15.53	1.530	.0717	14444	294	0		
	32 Spoke	1401	583.7	941	19.40	1.977	.0769	16091	293	51.2	NF
		1402	541.9	901	18.35	1.839	.0762	15547	295	51.5	
		1403	439.5	823	15.18	1.536	.0714	14569	297	51.2	
		1404	577	873	19.36	2.058	.0720	15970	298	76.2	
		1405	541.6	890	18.08	1.852	.0755	15394	299	76.8	
		1406	445	821	14.89	1.556	.0710	14494	302	76.8	
32 Spoke	1407	597.7	939	19.06	2.052	.0751	15796	304	93.6	NF	
	1408	548	894	17.65	1.876	.0741	15292	307	93.9		
	1409	443	807	14.54	1.563	.0695	14348	308	94.2		

TABLE II.— ISOLATED NACELLE WIND TUNNEL TEST

[Reverberation corrections for conical ejector nozzle and  
AIE auxiliary nozzle at an 18 ft (5.5 m) sideline]

Angle <sup>a</sup> (deg) freq. (Hz)	159°	149°	130°	120°	110°	101°	81°	61°	41°	30°
50	3 <sup>b</sup>	0	2.0	3.0	2.5	4.0	7.0	6.0	10.5	16.0
63	4	0	1.0	-1.5	1.0	3.5	4.0	6.5	10.5	15.0
80	1.5	.5	-4.5	.5	4.0	7.5	8.0	10.0	9.0	15.0
100	2.0	-7.0	0	4.5	6.5	9.5	12.0	13.5	15.0	13.5
125	7.5	-7.0	3.0	7.0	10.0	12.0	14.5	16.5	19.0	20.0
160	6.5	2.0	3.0	6.0	8.0	11.0	12.5	15.5	19.0	21.5
200	7.0	4.5	3.0	2.5	3.5	8.0	10.5	12.0	17.5	20.0
250	7.0	6.5	-4.5	1.0	7.0	10.5	11.0	14.5	10.0	17.5
315	9.5	-1.5	3.0	3.5	6.0	7.0	7.5	12.0	17.5	12.0
400	8.0	4.5	-2.0	5.0	7.5	10.0	9.5	14.5	16.5	21.0
500	9.0	4.5	1.0	3.0	6.5	8.5	9.0	11.0	16.0	18.5
630	8.5	4.5	1.0	3.0	6.0	7.0	7.5	11.0	12.0	18.0
800	10.0	5.0	1.0	4.5	5.0	7.0	9.5	9.0	14.5	13.5
1000	10.0	6.0	1.5	2.0	5.5	7.0	9.0	8.5	12.0	11.5
1250	13.5	7.5	1.0	2.5	5.0	6.0	7.5	10.5	11.5	13.0
1600	12.0	7.5	.5	1.5	4.5	5.5	7.6	9.0	9.5	20.0
2000	15.0	9.5	2.0	2.5	4.5	6.0	7.0	8.5	10.5	16.5
2500	15.0	10.0	2.5	4.0	4.5	5.0	6.5	9.0	11.5	13.5
3150	17.0	10.0	1.5	2.5	2.0	4.0	5.5	7.5	9.5	13.0
4000	13.5	10.0	1.5	.5	1.0	3.0	5.0	5.5	9.0	12.0
5000	14.5	10.0	.5	1.0	1.0	2.5	4.0	4.5	8.5	10.0
6300	14.5	10.0	.5	.5	1.0	1.5	3.5	4.0	8.5	6.5
8000	14.0	11.0	0	1.0	0	.5	2.0	3.0	5.5	1.0
10000	12.5	10.0	-1.5	-1.0	-2.0	-2.0	2.0	1.5	5.5	-1.0

<sup>a</sup> Angle is reference to inlet.

<sup>b</sup>  $\Delta SPL$ -dB.

TABLE III.— WING NACELLE WIND TUNNEL TEST

[Reverberation corrections for conical ejector nozzle]

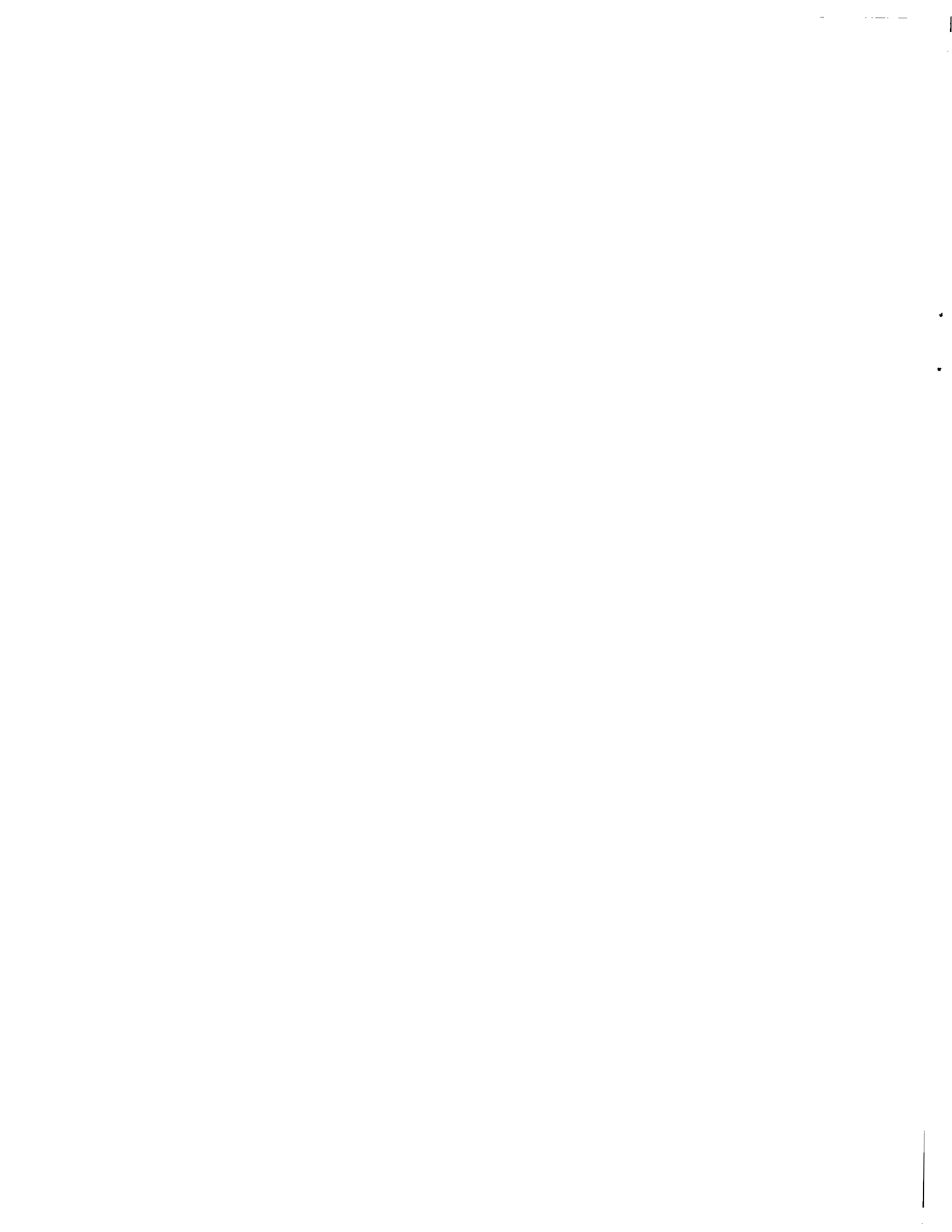
Angle <sup>a</sup> (deg) freq. (Hz)	162°	147°	127°	111°	101°	90°	70°
50	2.0 <sup>b</sup>	-3.3	-2.2	-0.4	3.4	2.9	2.4
63	1.2	-9.3	0.5	1.3	4.3	4.3	5.2
80	1.4	-4.3	6.2	4.7	7.1	7.2	7.7
100	9.5	0.6	7.6	5.1	6.8	6.5	8.0
125	5.1	3.8	9.3	6.6	7.0	6.3	7.9
160	2.9	4.3	2.6	4.7	7.7	8.1	8.1
200	5.0	-5.2	7.1	5.6	6.8	6.5	9.5
250	5.9	2.2	3.8	2.2	3.1	3.9	3.6
315	-2.5	0.3	6.8	3.7	4.1	3.9	5.7
400	7.0	3.4	5.7	4.2	5.6	5.4	7.5
500	6.1	2.5	6.3	3.8	5.2	5.7	6.9
630	7.6	2.8	4.6	4.1	4.1	4.5	6.1
800	8.1	1.9	5.6	3.0	4.2	4.8	5.4
1000	9.5	4.3	4.6	2.2	4.6	3.9	4.3
1250	10.0	4.5	5.2	3.1	4.3	4.0	4.6
1600	11.5	5.3	4.4	3.1	3.8	4.3	5.3
2000	11.6	5.3	4.3	3.0	3.7	3.8	6.4
2500	12.1	5.9	3.9	2.8	4.2	3.7	6.4
3150	11.3	6.0	3.1	1.8	3.2	2.4	4.7
4000	10.3	5.3	3.1	1.1	3.0	2.0	4.2
5000	10.6	5.1	2.9	0.2	2.0	2.5	3.4
6300	10.3	4.1	2.3	-0.4	0.7	0.9	1.8
8000	9.5	3.9	2.1	-1.1	-1.1	-1.3	-0.2
10000	8.5	3.4	1.1	-3.7	-1.1	-0.3	-0.9

<sup>a</sup>Angle is reference to inlet.

<sup>b</sup> $\Delta$ SPL-dB.

TABLE IV.— SUMMARY OF FIGURES 15, 16, AND 17

Nozzle configuration	Suppression relative to conical peak noise angle	Directivity change with wing	
Conical ejector	0	40° – 90° 1 – 3 PNdB increase	90° – 150° 1 – 2 PNdB decrease
AIE	-1 PNdB	—	—
32 spoke	7 PNdB	40° – 70° 1 – 2 PNdB increase	80° – 150° 1 PNdB decrease
104 tube without shroud	11 PNdB	—	—
104 tube with shroud	17 PNdB	40° – 80° 1 PNdB increase	90° – 150° 2 – 3 PNdB at peak decrease



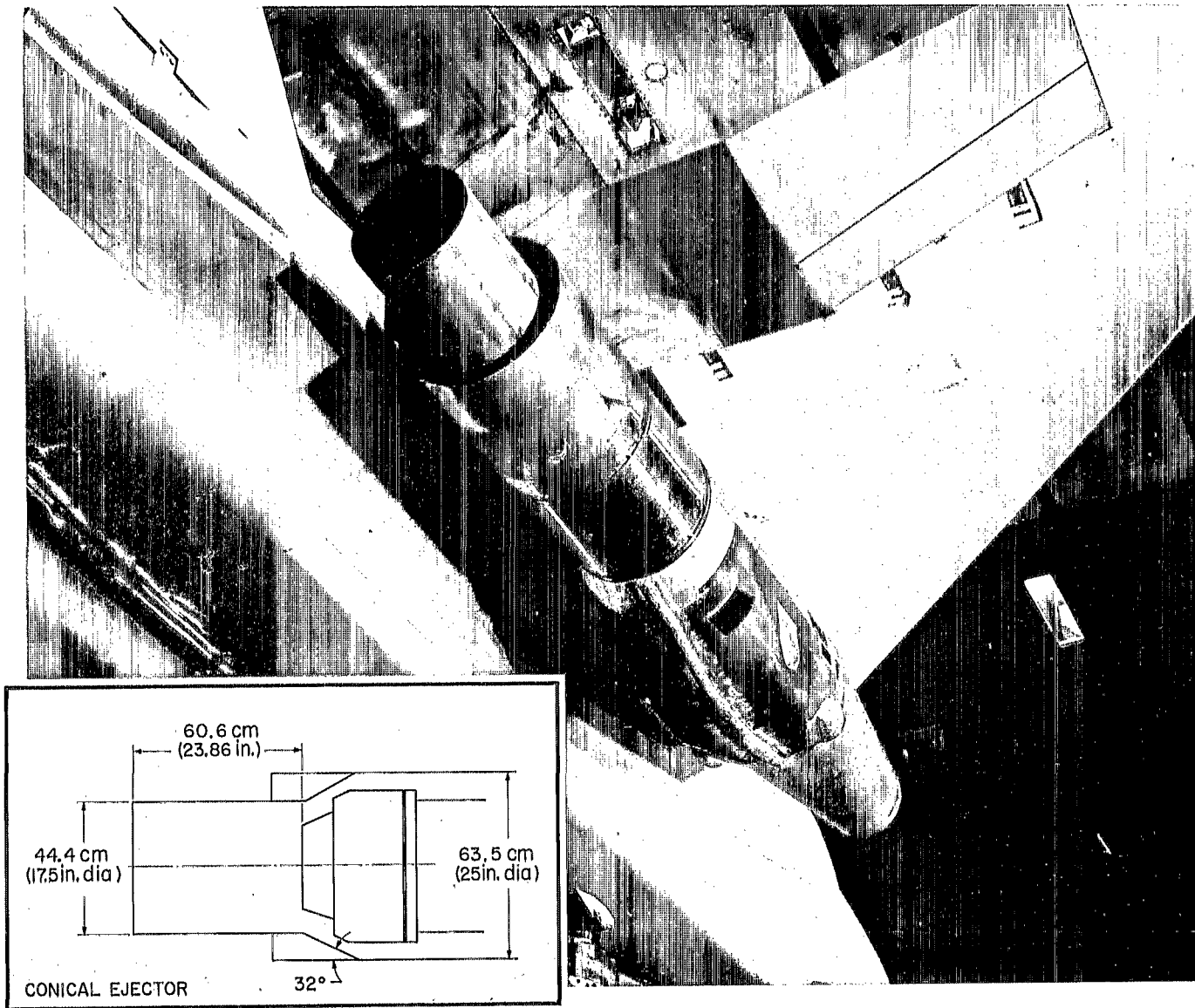


Figure 1.-- Schematic drawing of conical ejector nozzle installed under the wing.

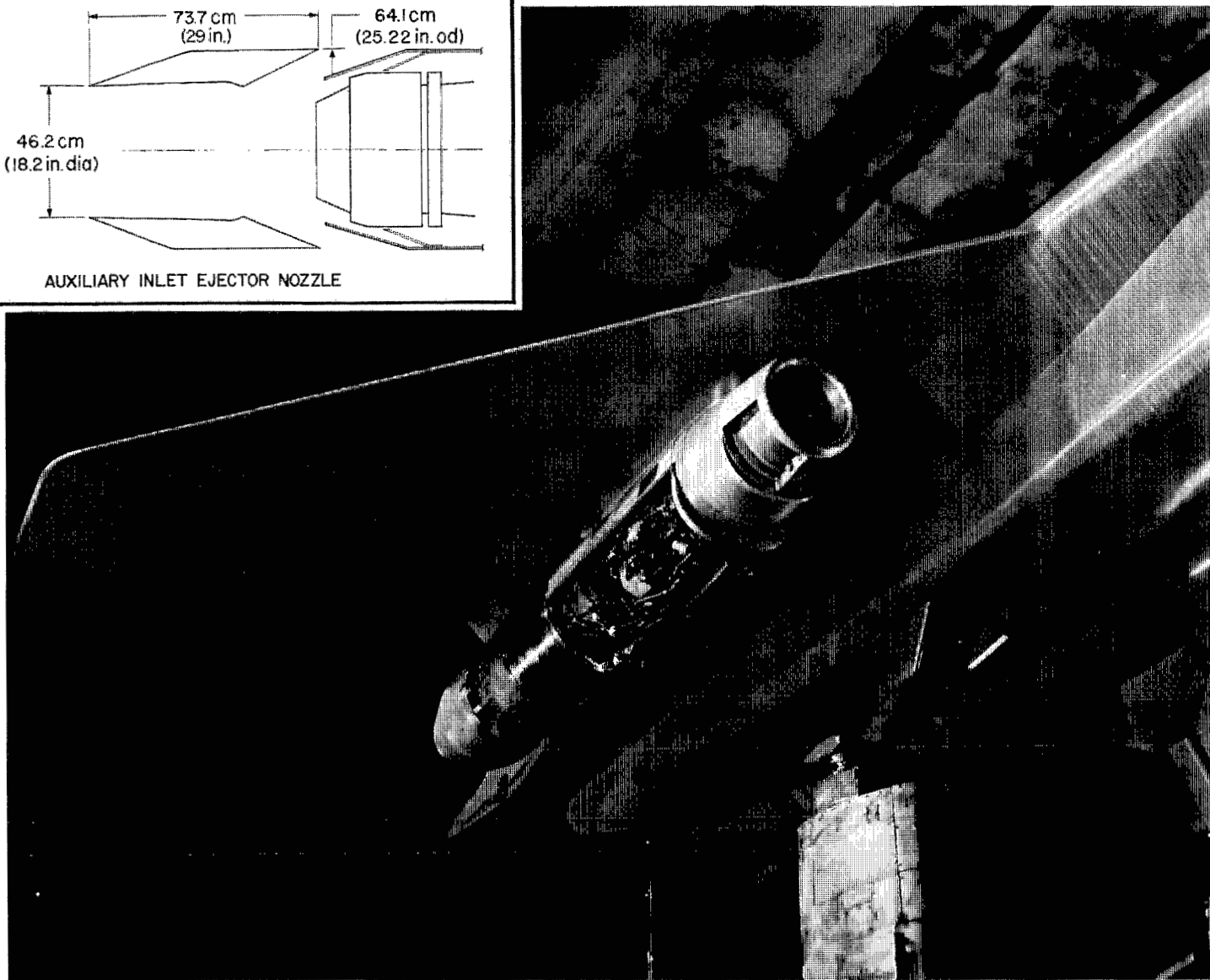
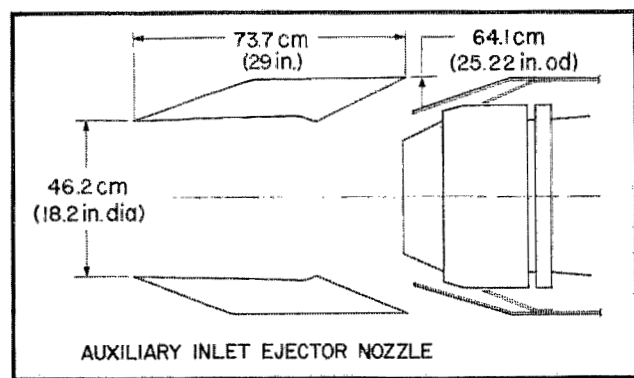


Figure 2.— AIE nozzle under wing installation with bellmouth inlet.

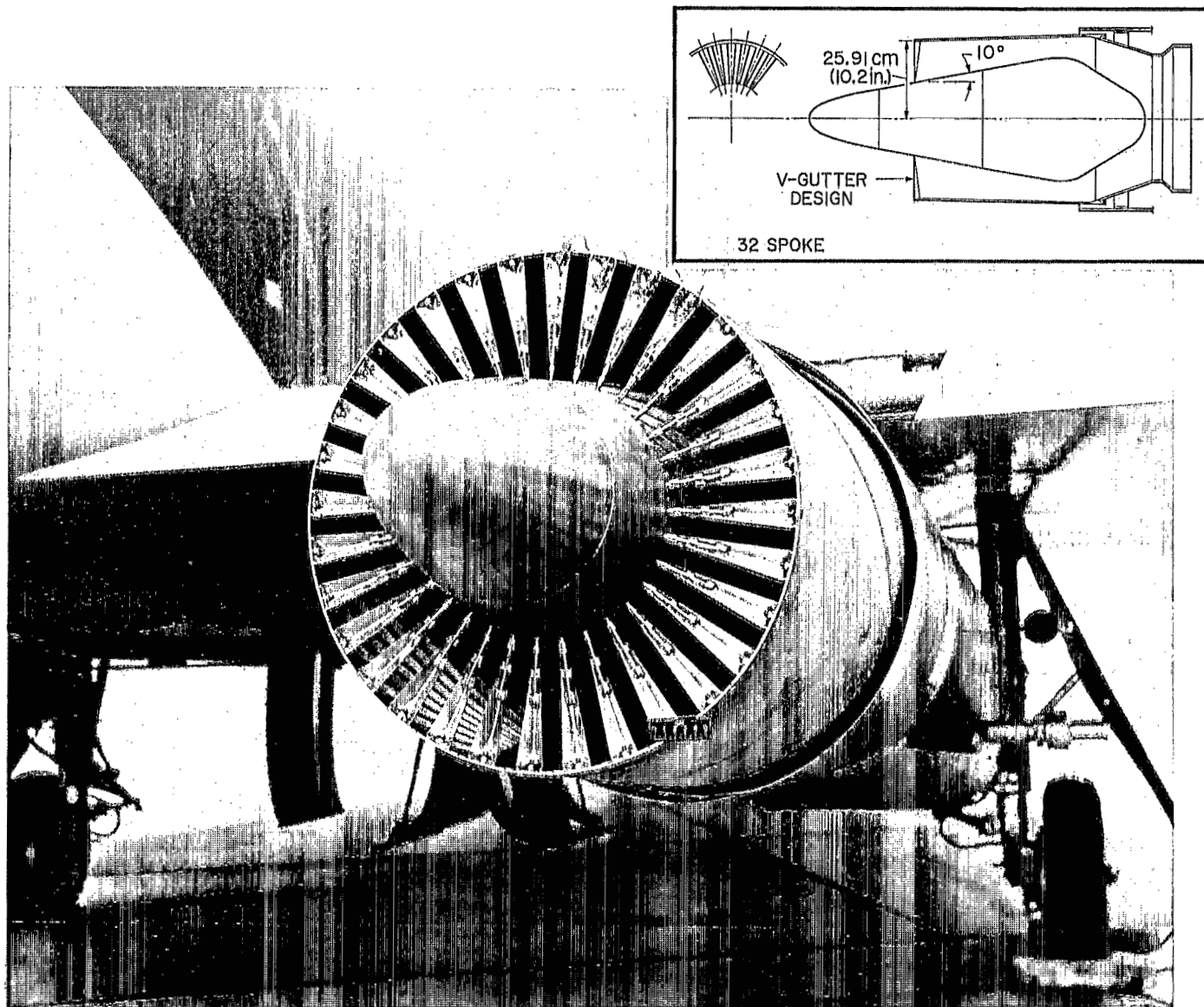


Figure 3.— Schematic drawing of 32-spoke area ratio nozzle.

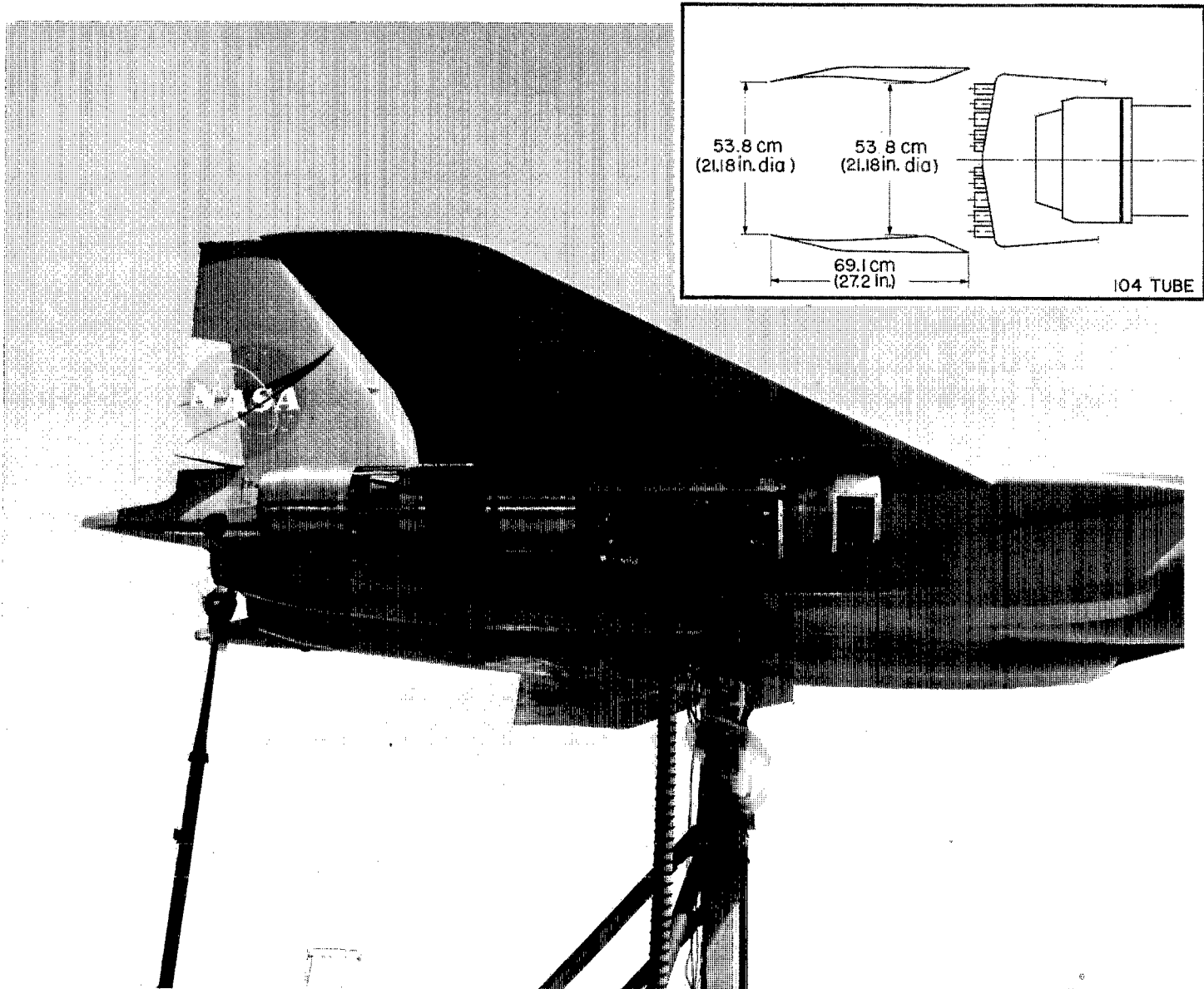
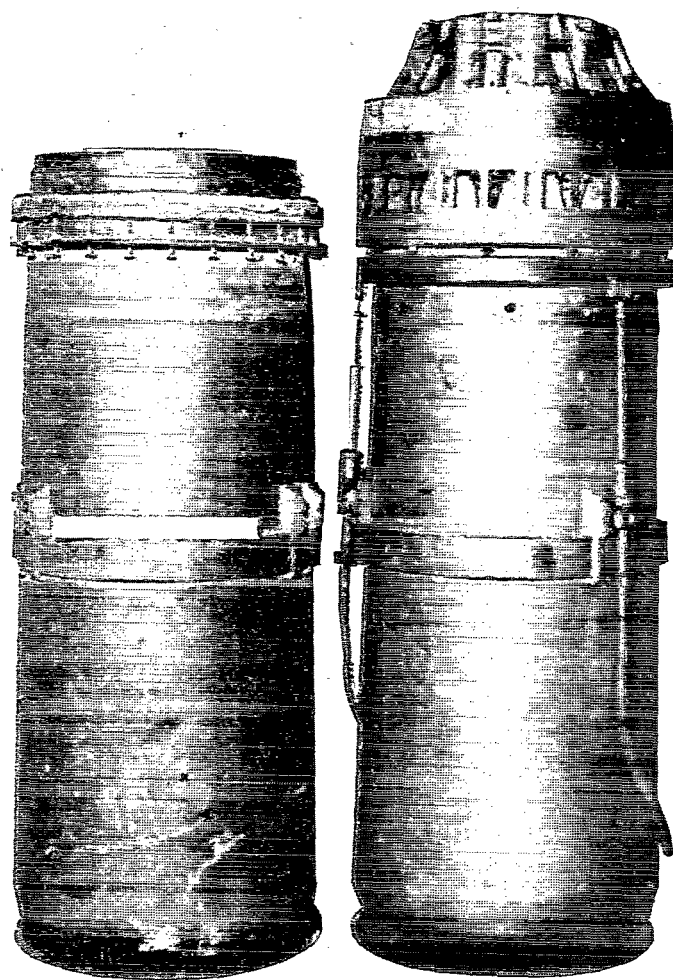


Figure 4.— 104-tube nozzle under wing installation outdoor static test.



(a) Fixed area  
nozzle exit.

(b) Variable area  
nozzle exit.

Figure 5.— Afterburner cans.

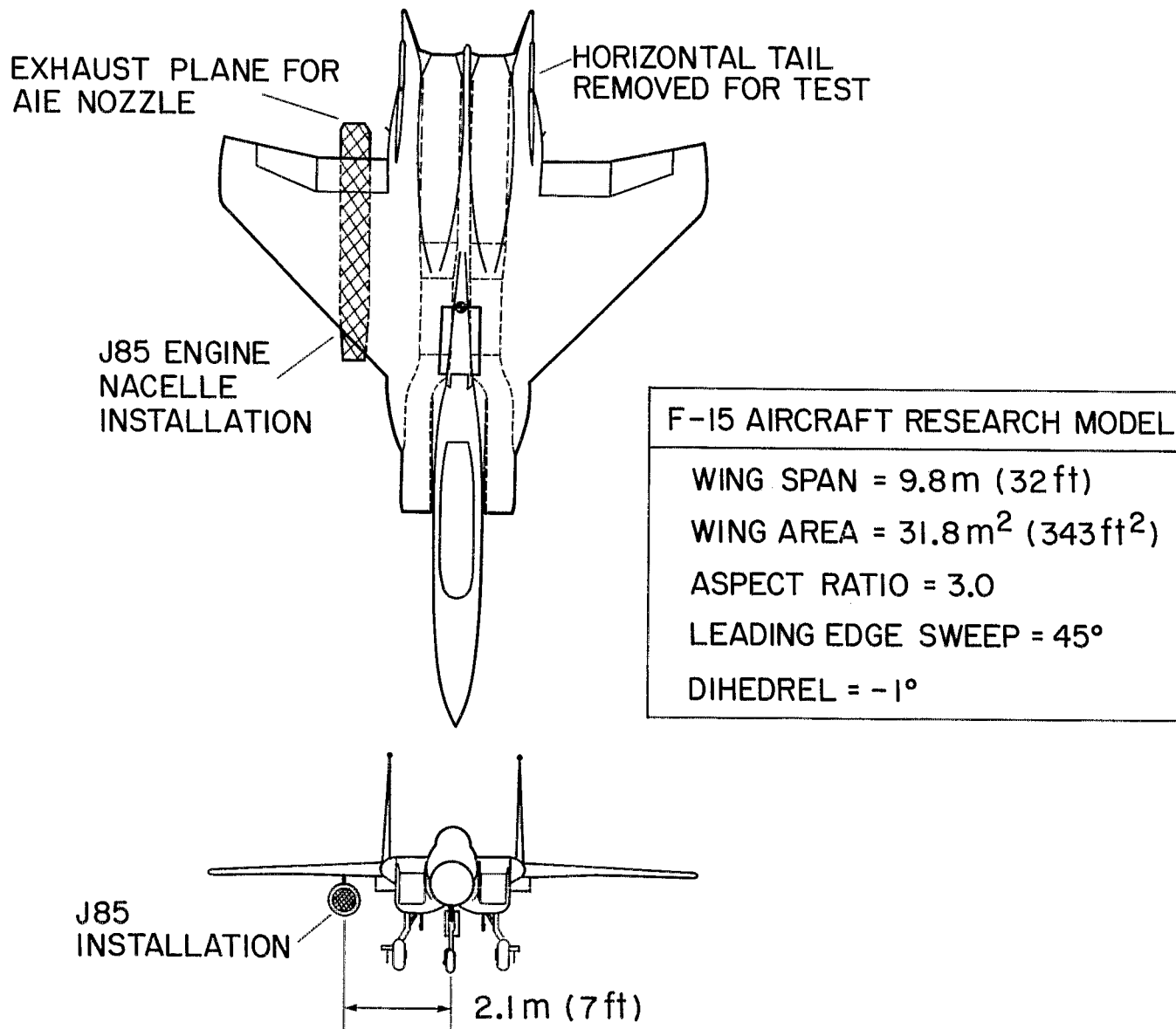


Figure 6.— Schematic drawing of F-15 3/4-scale research aircraft model.

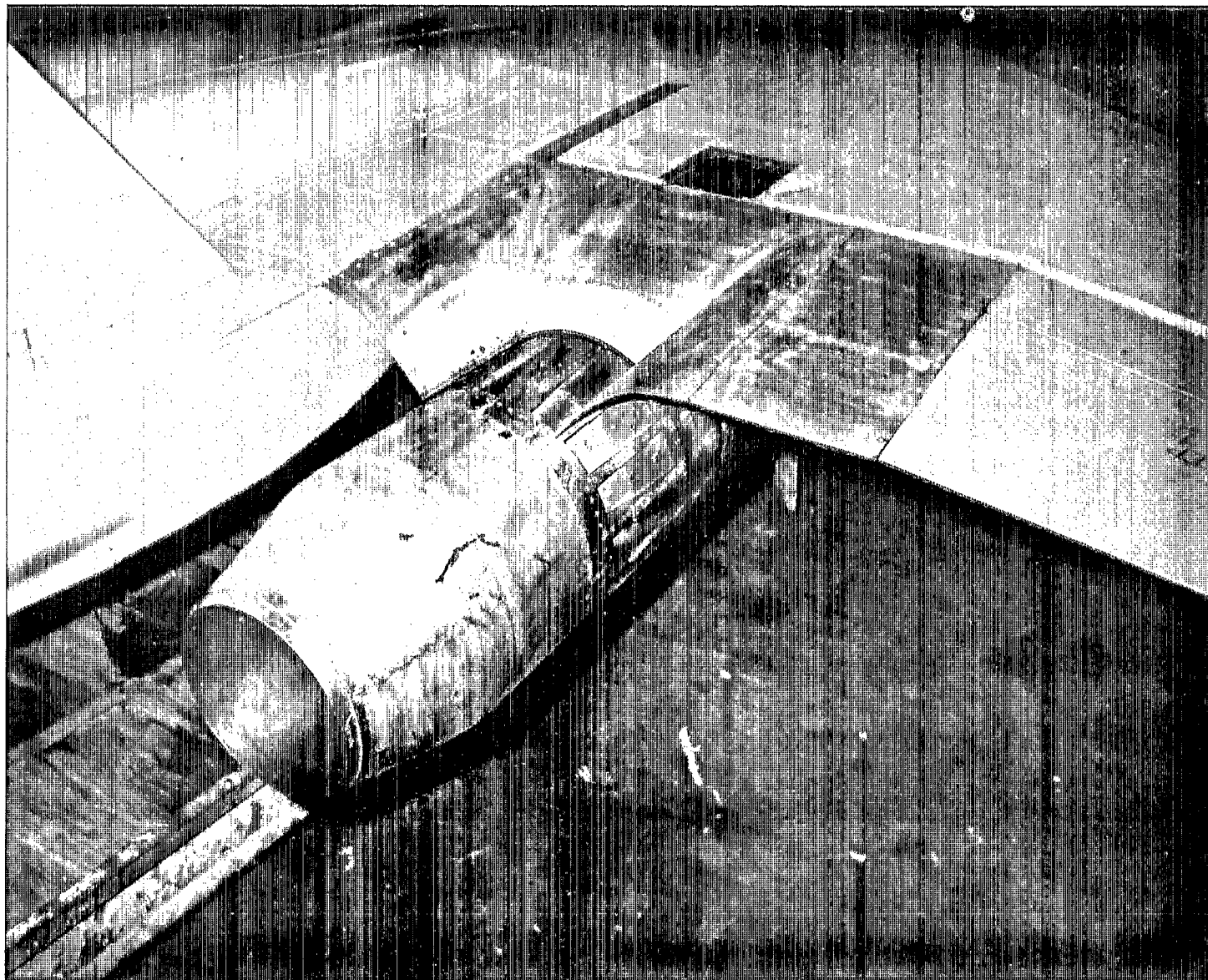


Figure 7.— Flap installation for AIE nozzle.



Figure 8.— Isolated nacelle installation, static test.

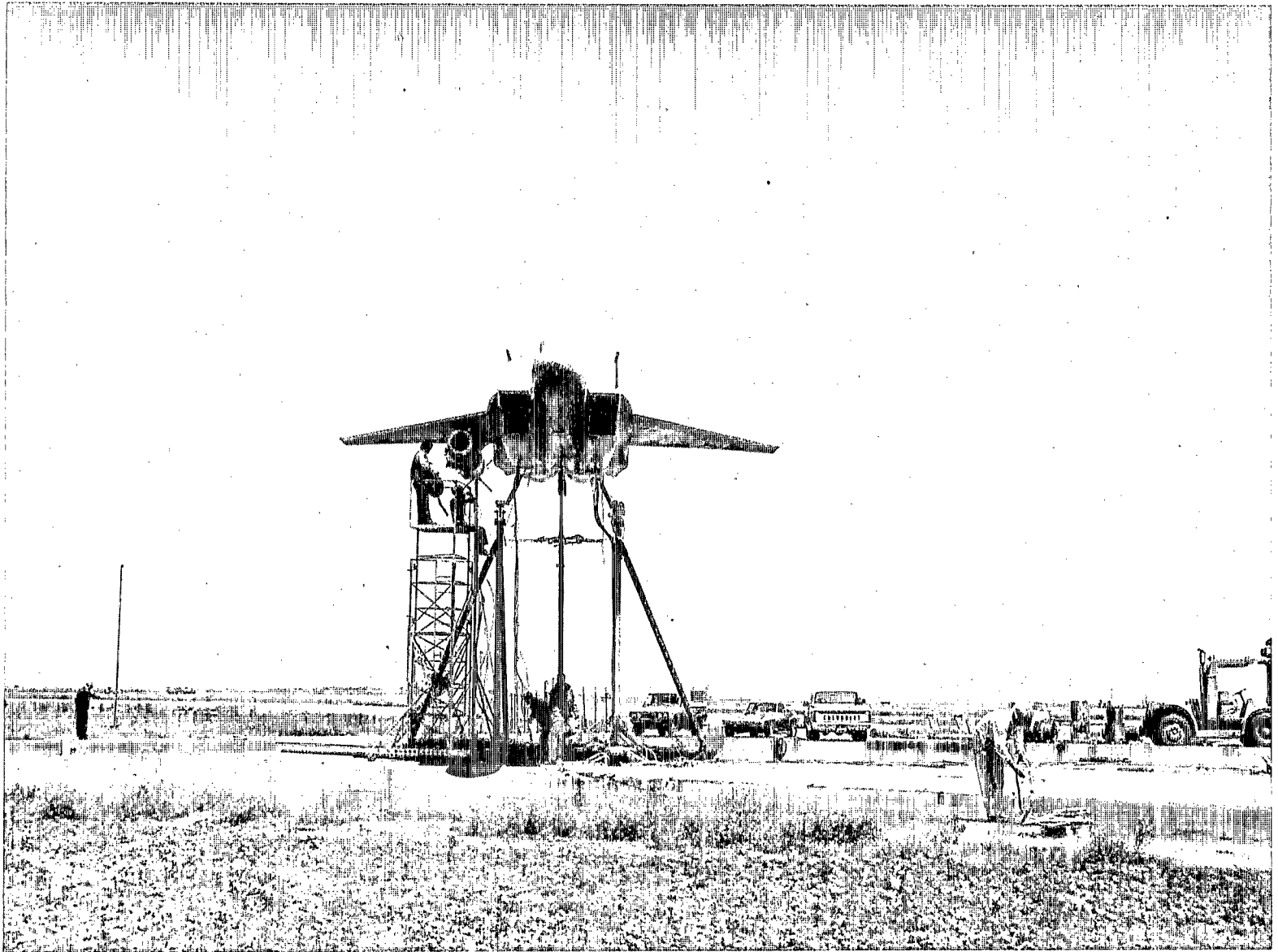


Figure 9.— Nacelle under wing installation, static test.

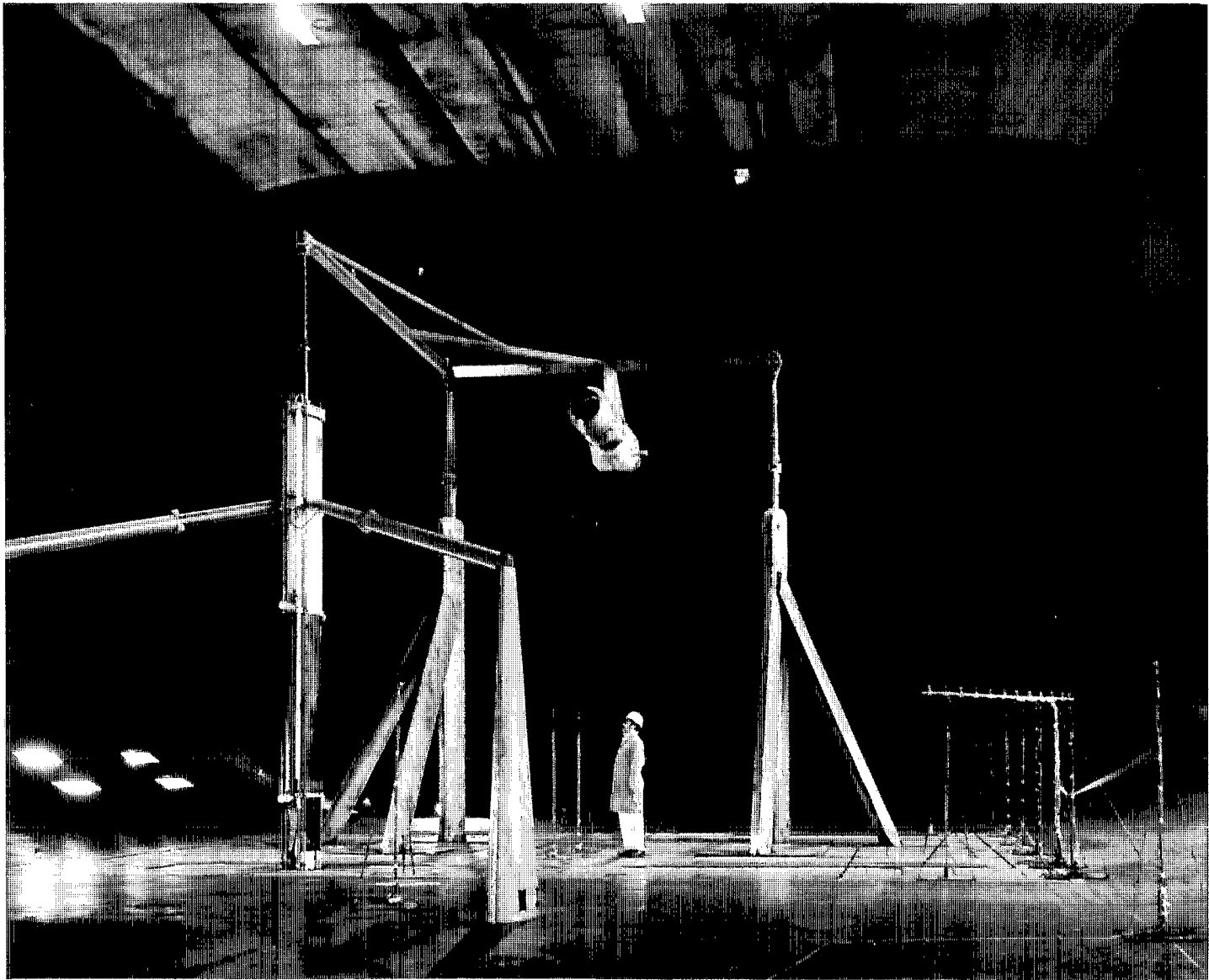


Figure 10.— Isolated nacelle installation, wind tunnel.

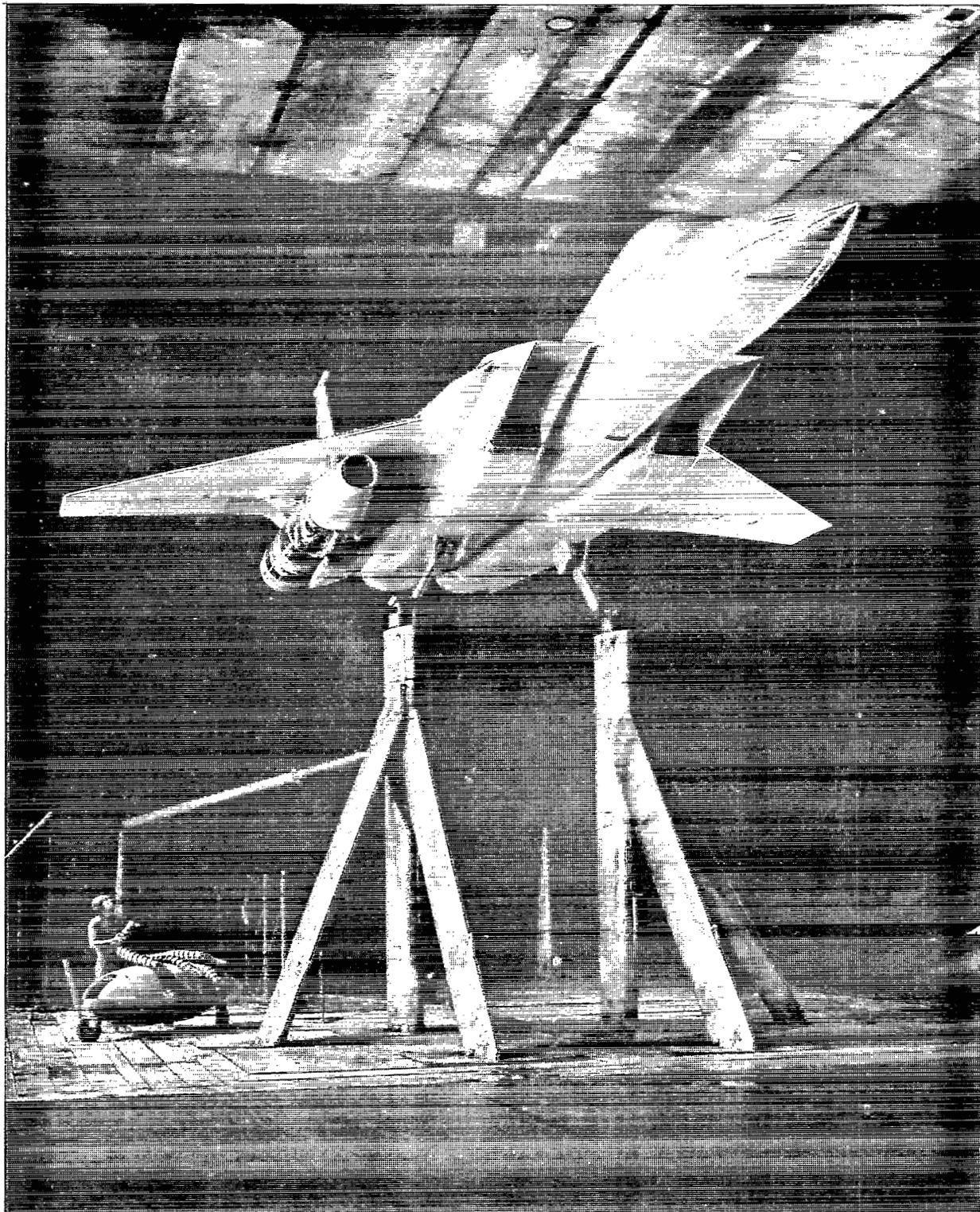
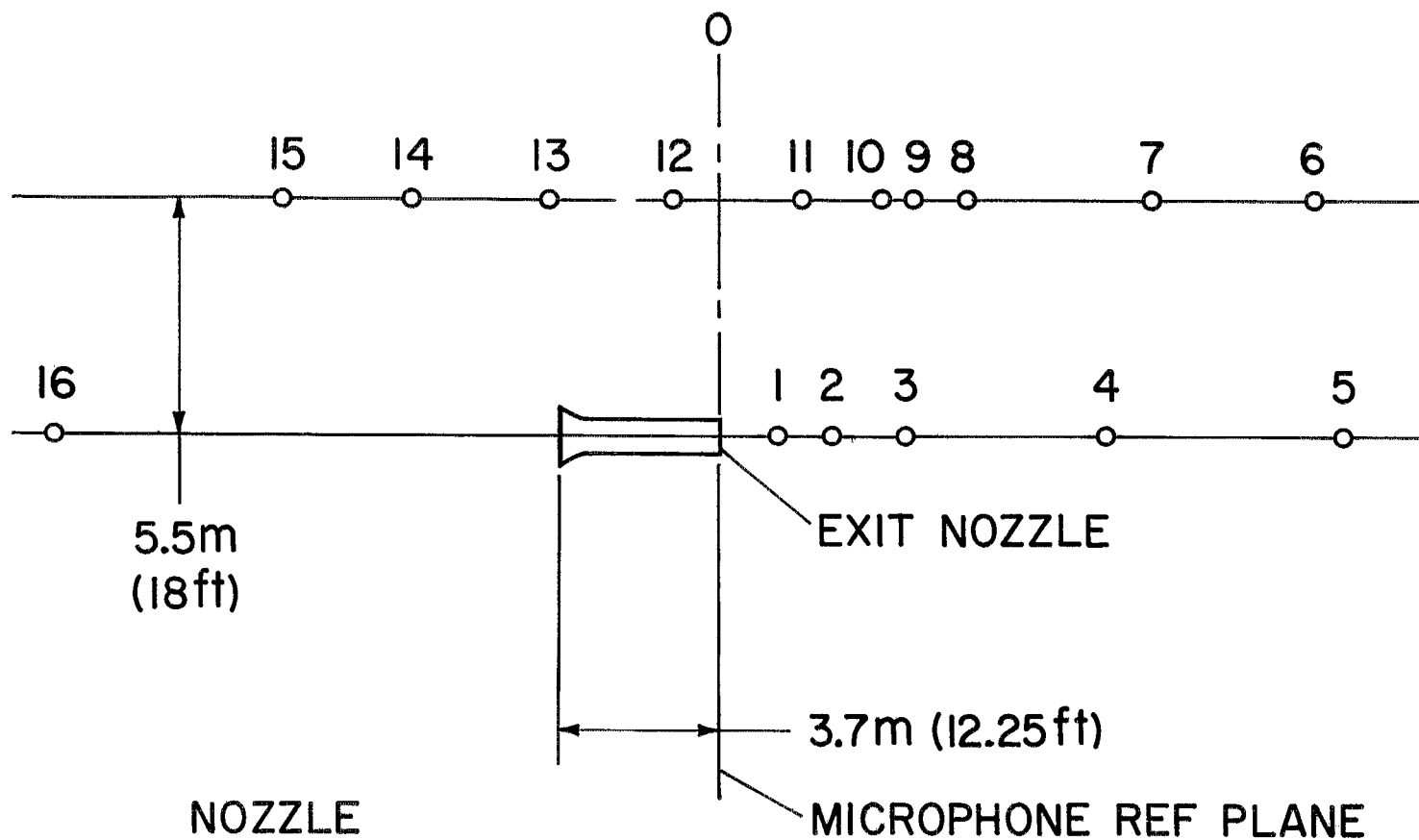


Figure 11.— Nacelle under wing installation, wind tunnel.



NOZZLE  
CONFIGURATION

CONICAL  
32 SPOKE  
104 TUBE WITH SHROUD  
104 TUBE WITHOUT SHROUD

MICROPHONE REF PLANE

PLAN VIEW

ALL MICROPHONE HEIGHTS  
1.8m (6ft) FROM GROUND

Figure 12.— Isolated nacelle outdoor static test and wind-tunnel microphone locations.

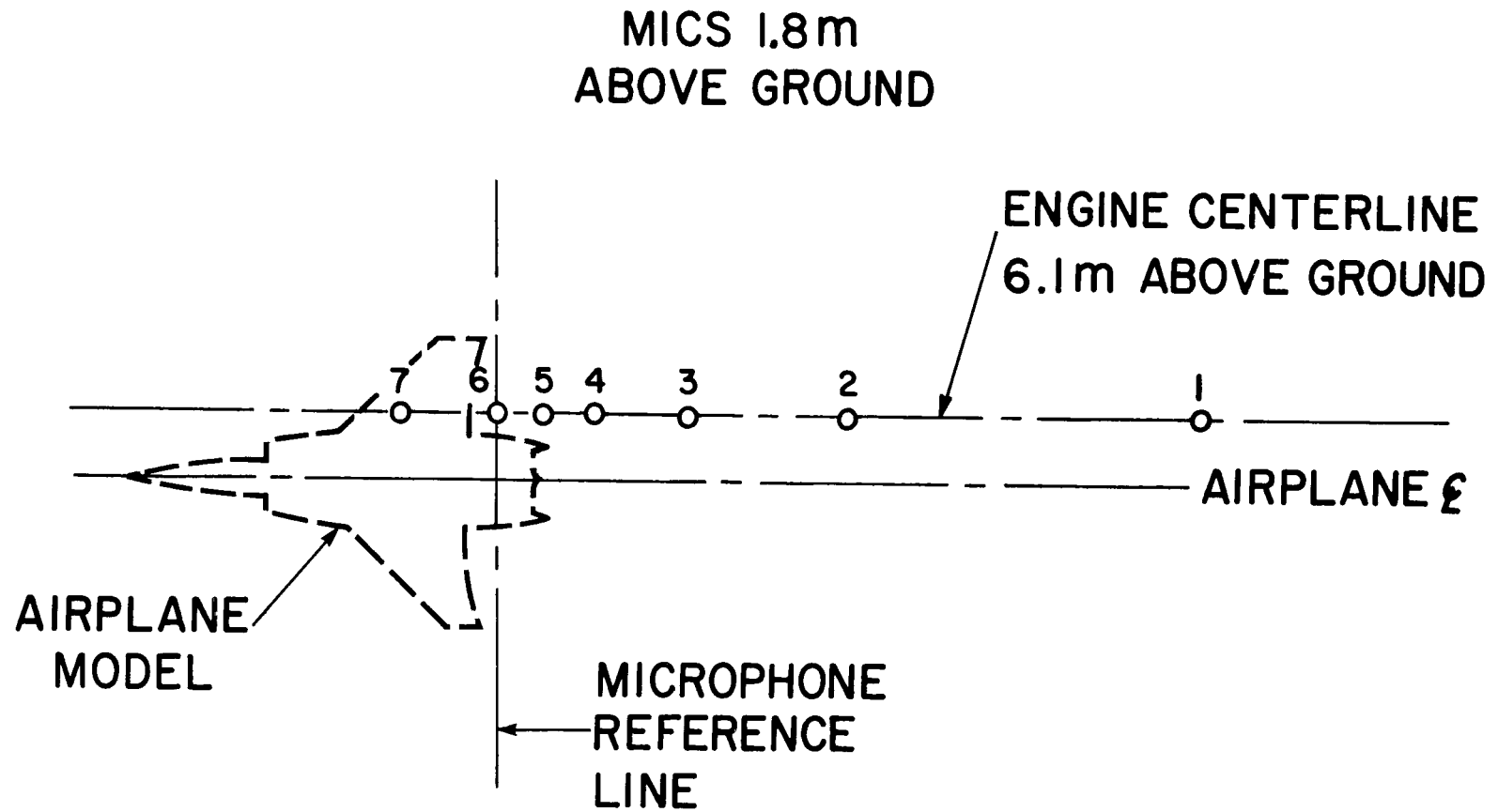


Figure 13.— Microphone positions for nacelle under wing installation for wind tunnel and for outdoor static test.

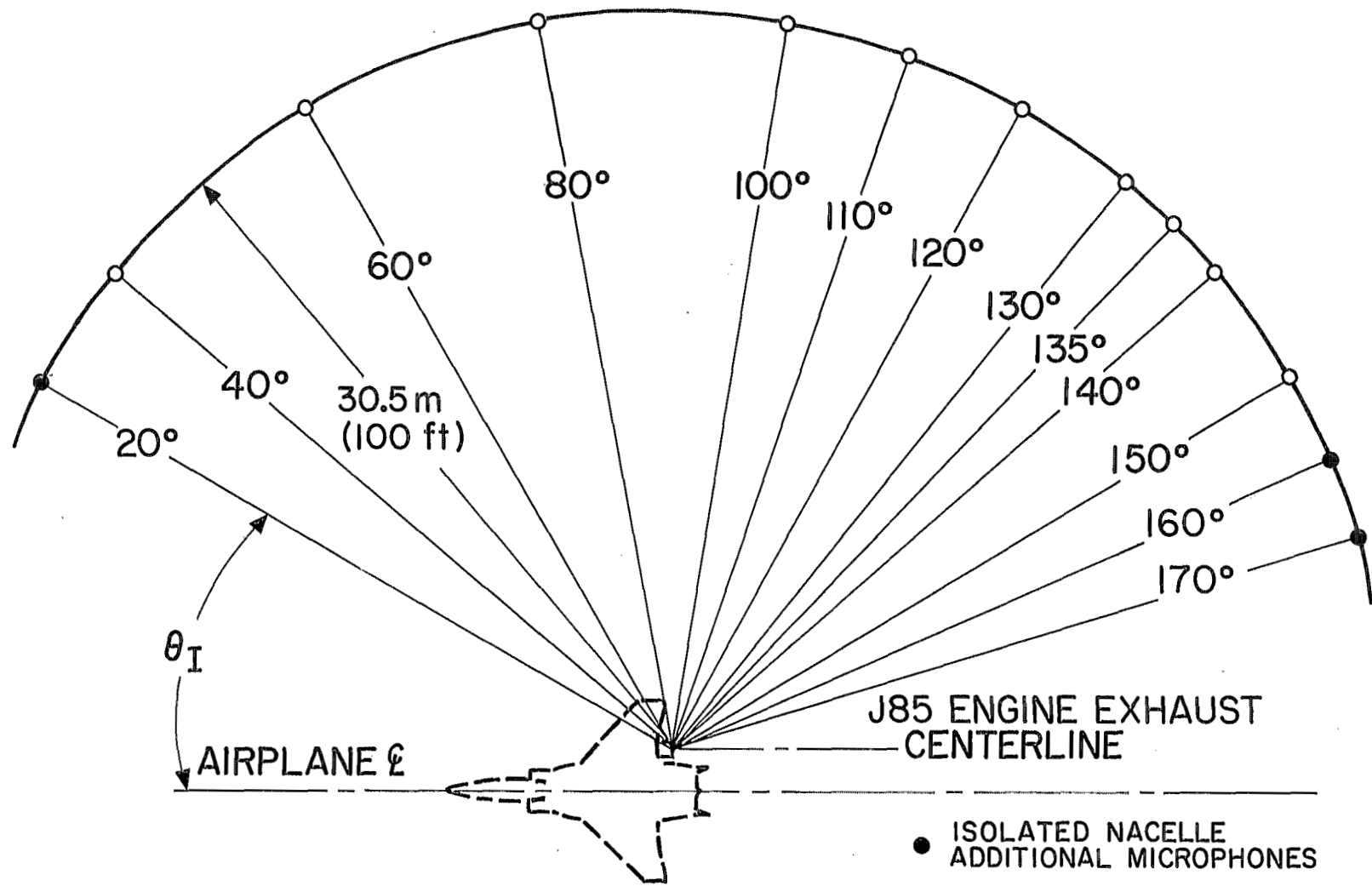


Figure 14.— Microphone locations of 30.5-m (100-ft) radius arc for outdoor static tests.

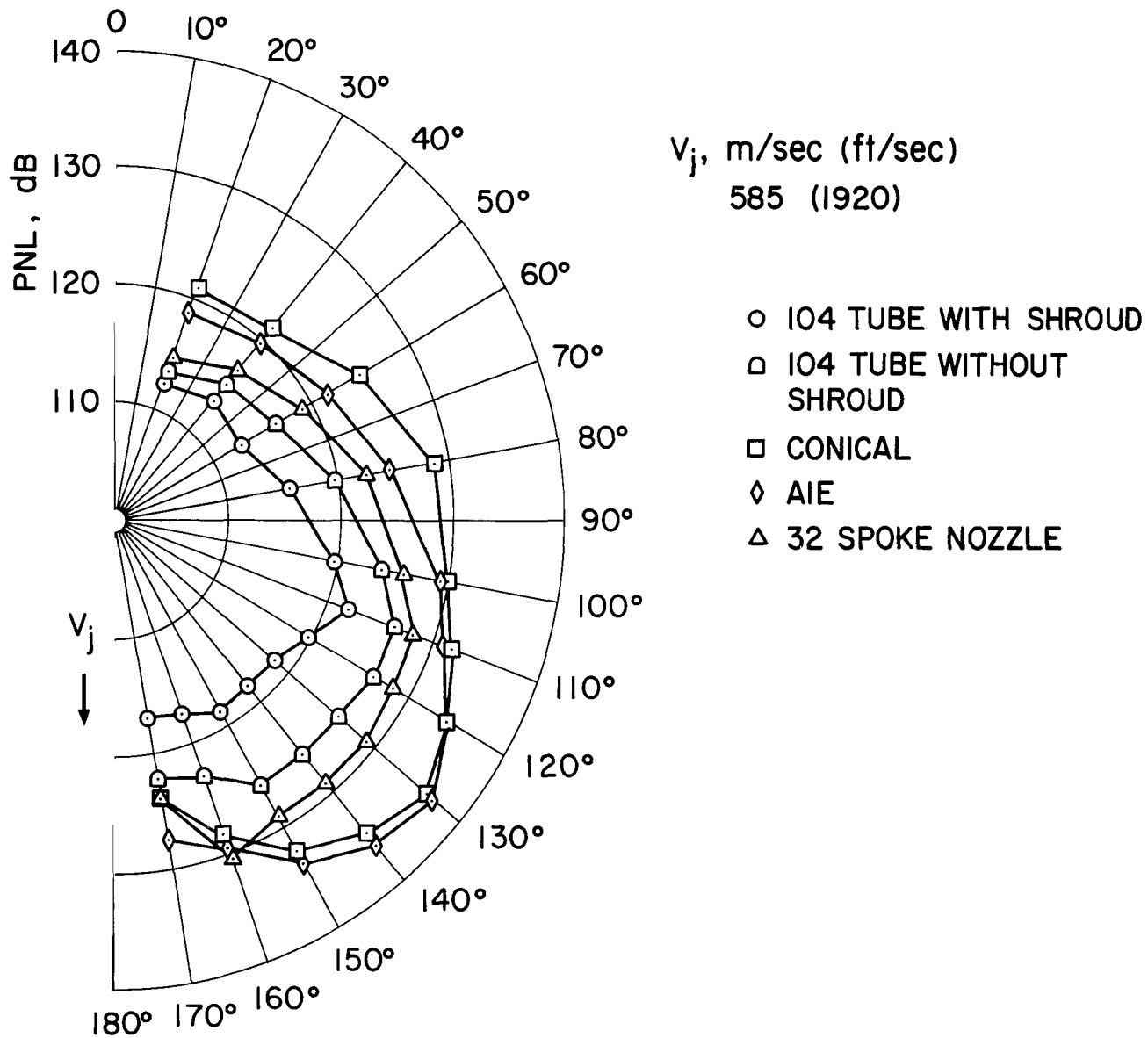


Figure 15.— PNL directivity for isolated nacelle installation outdoor static test; 30.5-m (100-ft) radius arc measurements.

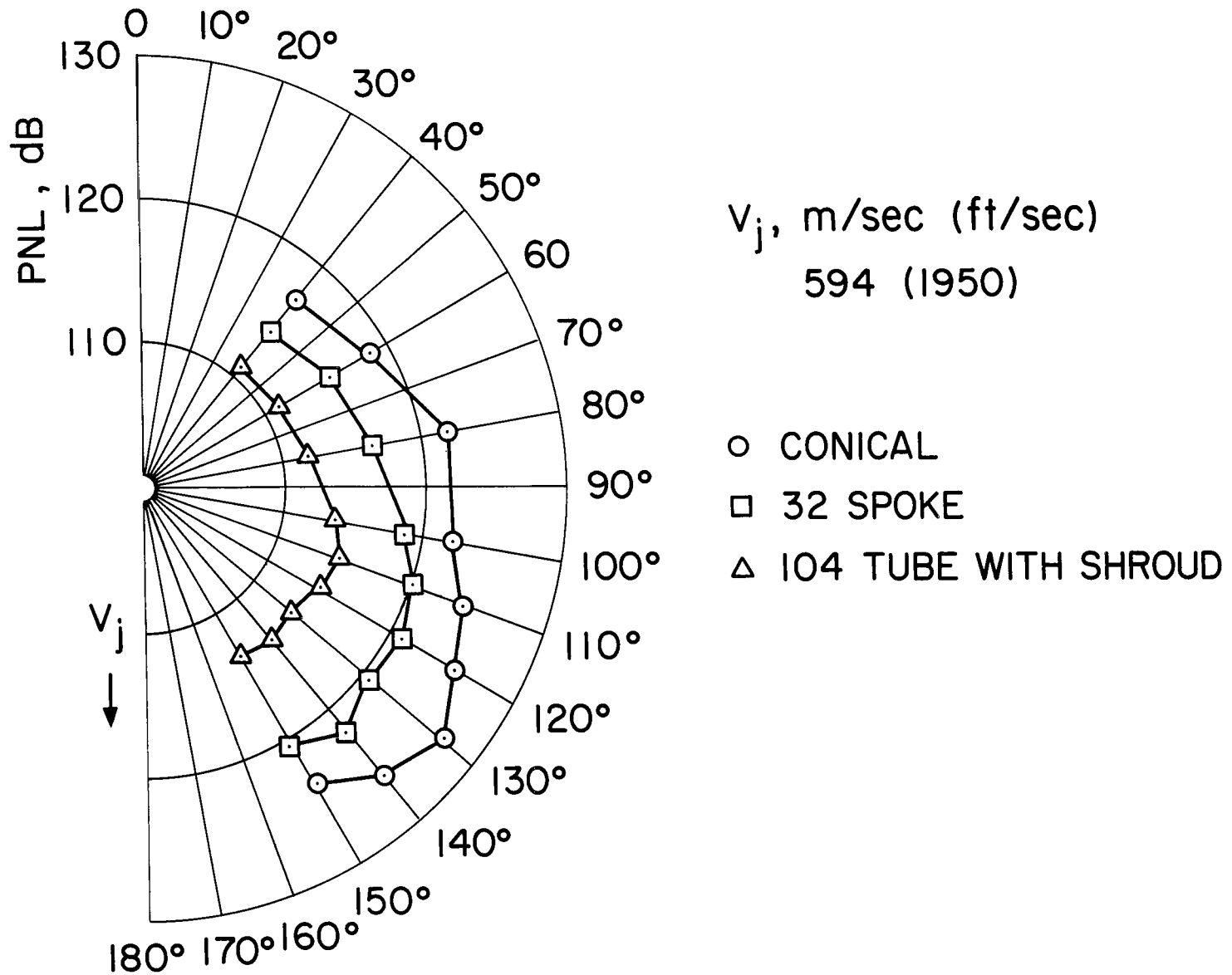


Figure 16.— PNL directivity for nacelle under wing installation outdoor static test, 30.5-m (100-ft) radius arc measurements.

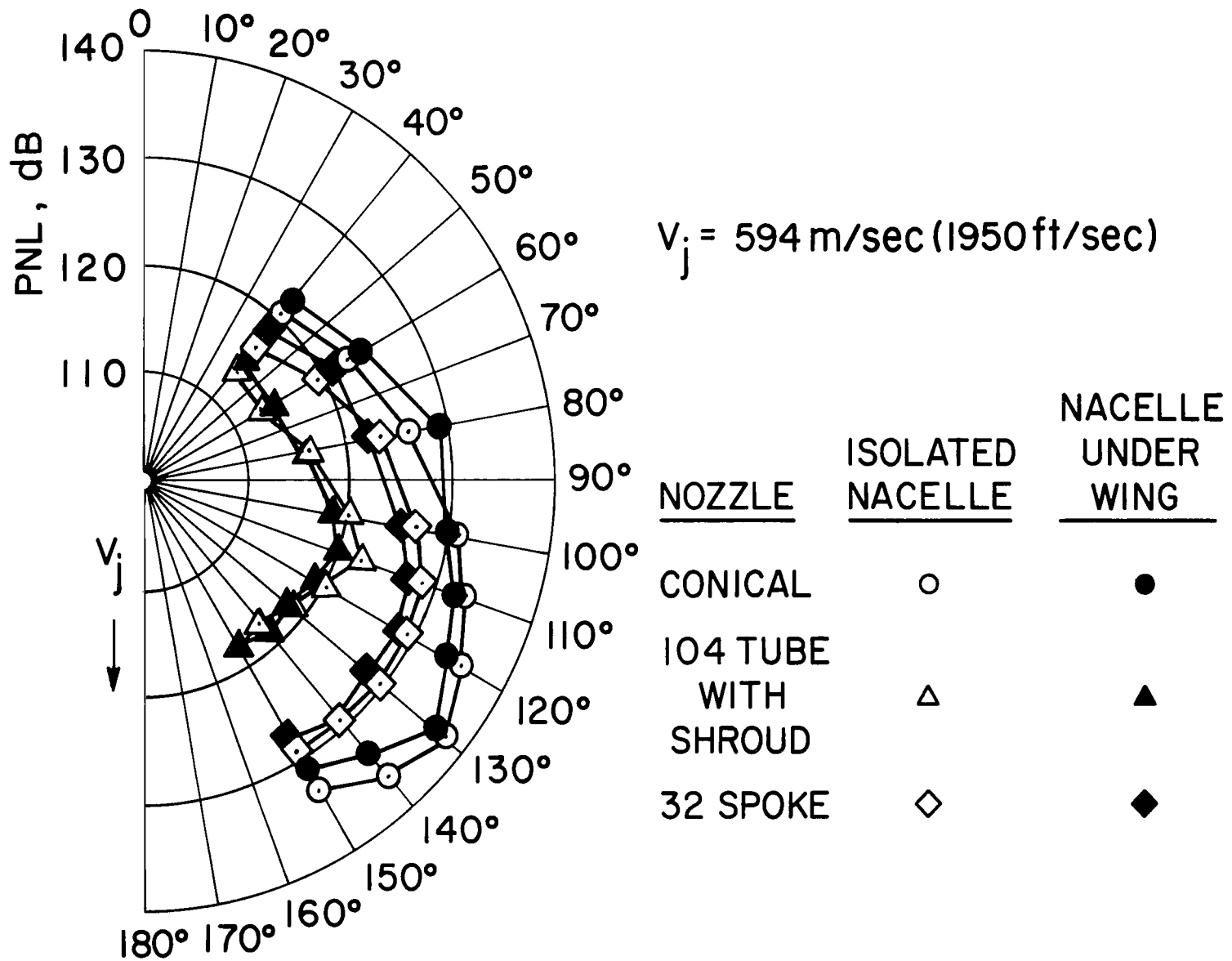


Figure 17.— Far-field PNL directivity for isolated nacelle vs nacelle under wing installation outdoor static test, 30.5-m (100-ft) radius arc measurements.

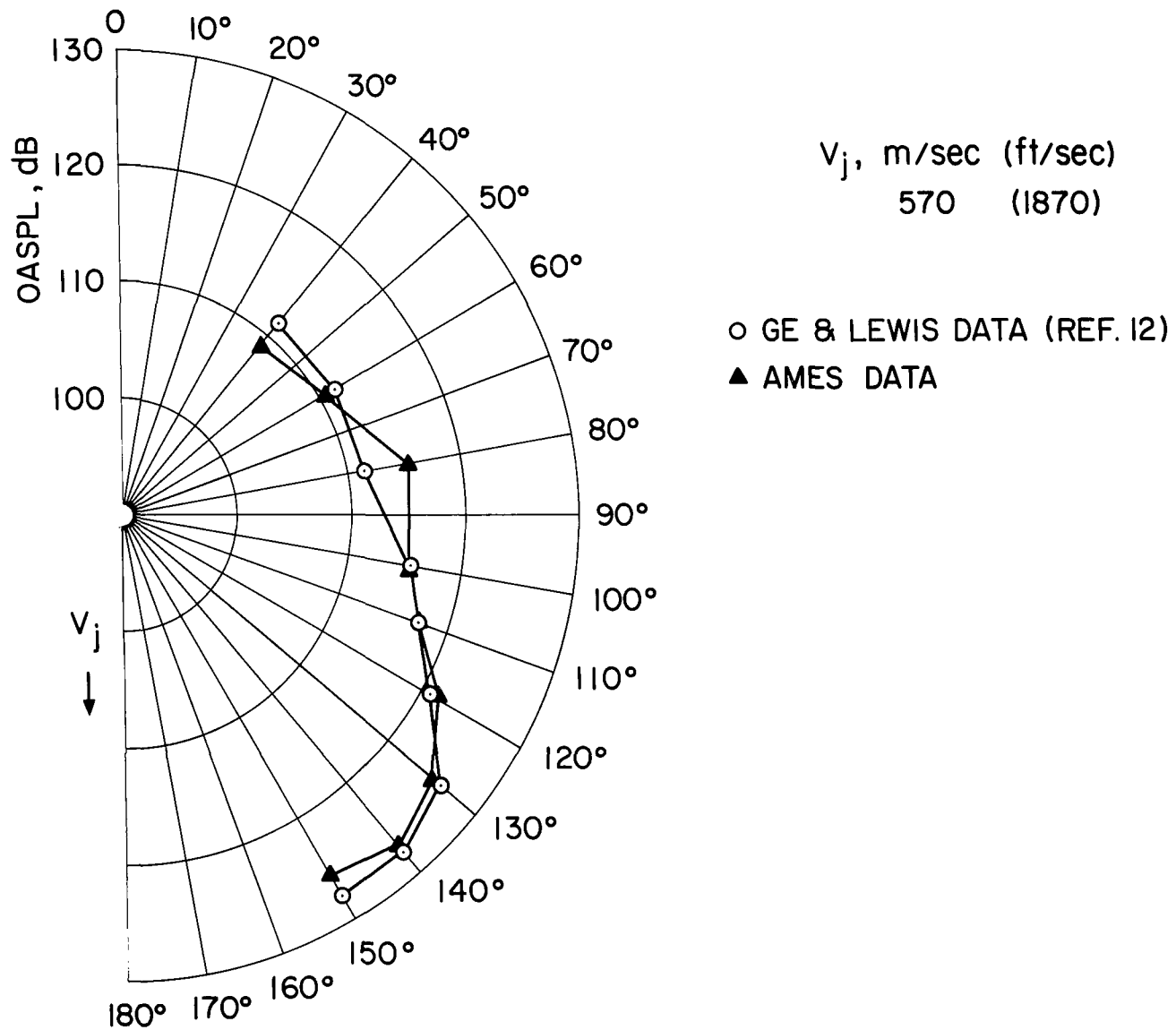


Figure 18.— Comparison of OASPL for conical nozzle under wing installation; Lewis Research Center data vs Ames data 30.5-m (100-ft) radius arc.

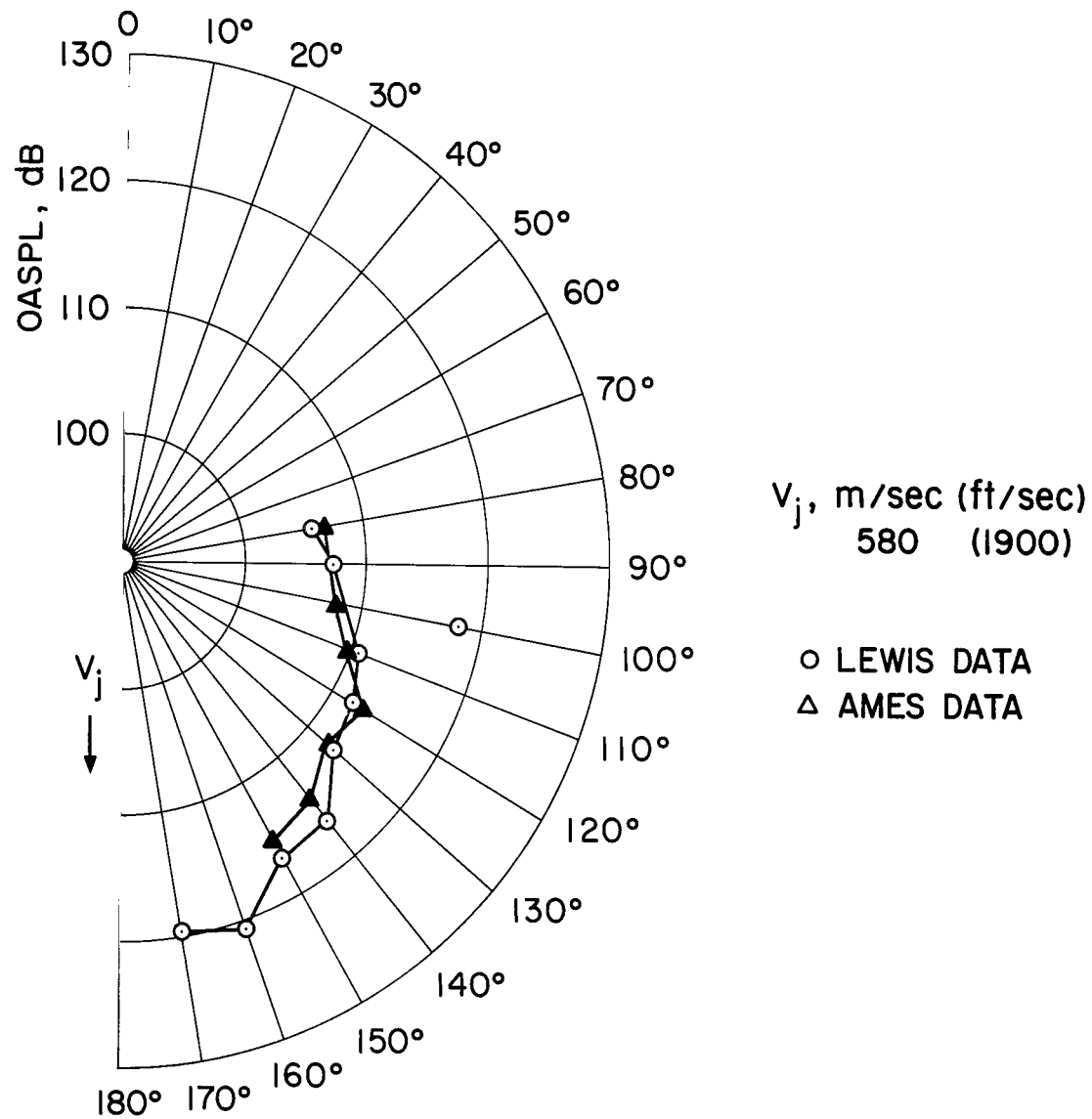


Figure 19.— Comparison of OASPL for 104-tube nozzle without acoustic shroud under wing installation; Lewis Research Center data vs Ames data, 30.5-m (100-ft) radius arc.

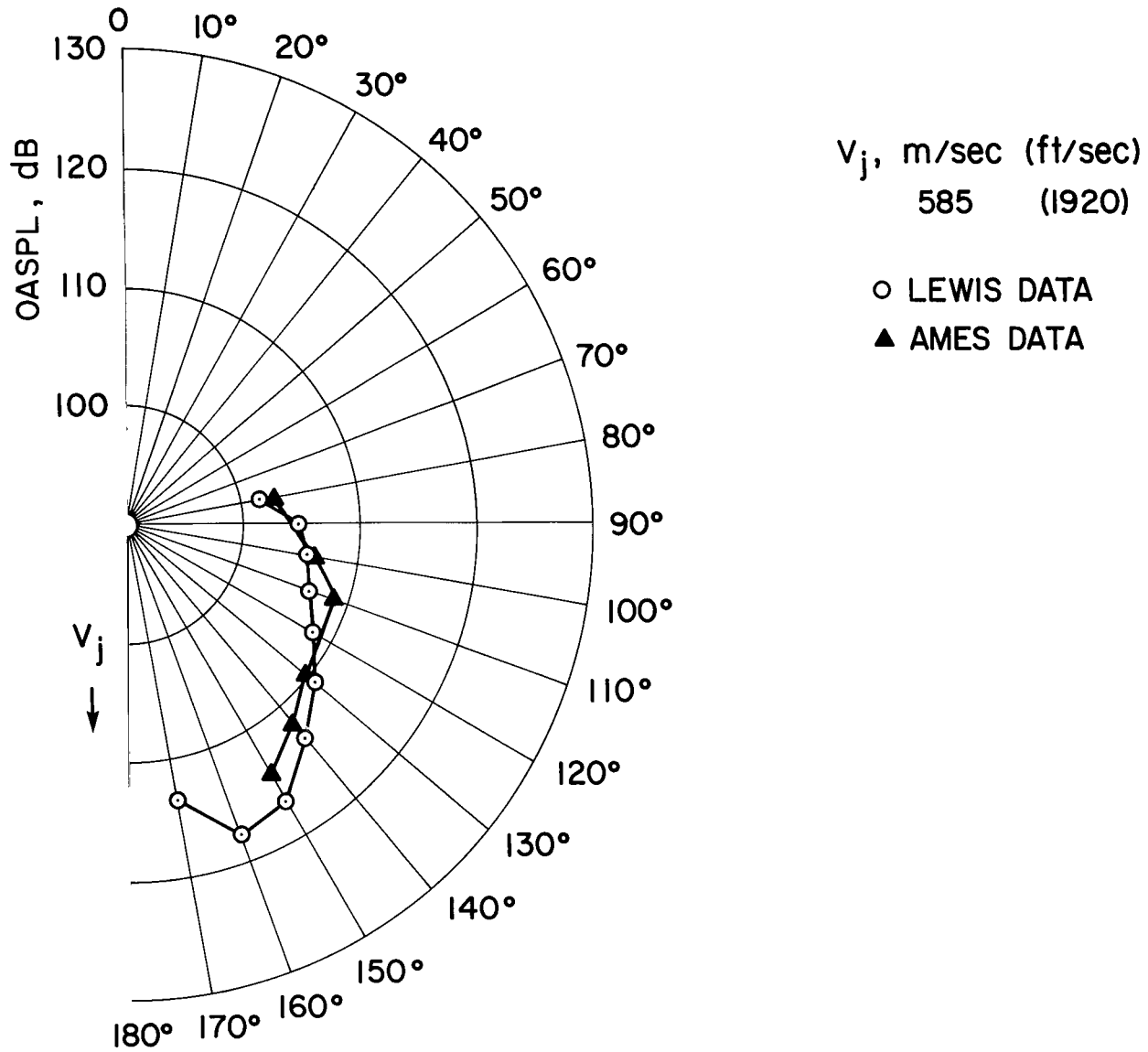


Figure 20.— Comparison of OASPL for 104-tube nozzle with acoustic shroud under wing installation; Lewis Research Center data vs Ames data.

59° F, 70% RELATIVE HUMIDITY  
 30.5m (100 ft) ARC  $V_j = 582 \text{ m/sec (1910 ft/sec)}$

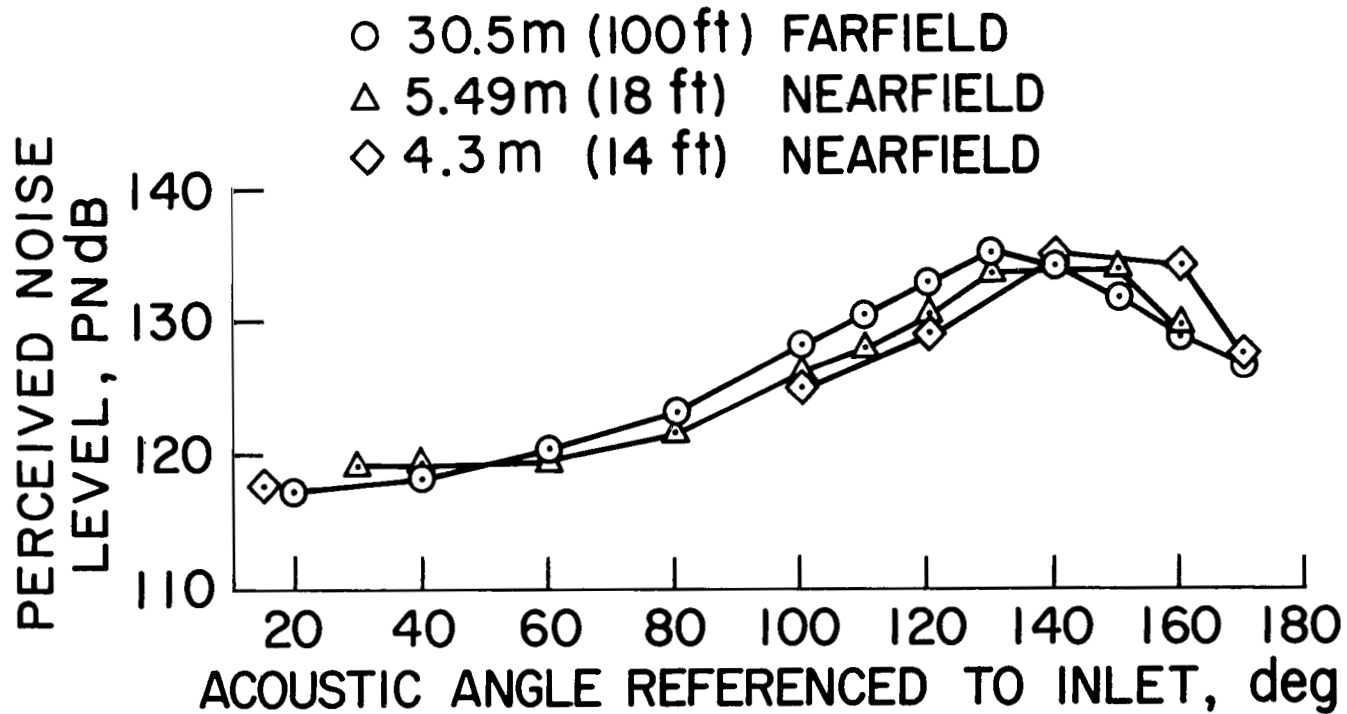


Figure 21.— Far-field to near-field comparison of PNL directivity for the conical ejector nozzle isolated nacelle installation, outdoor static test.

104 TUBE NOZZLE W/O SHROUD      59° F, 70% RELATIVE HUMIDITY  
 30.5 m (100 ft) ARC       $v_j = 605$  m/sec (1985 ft/sec)

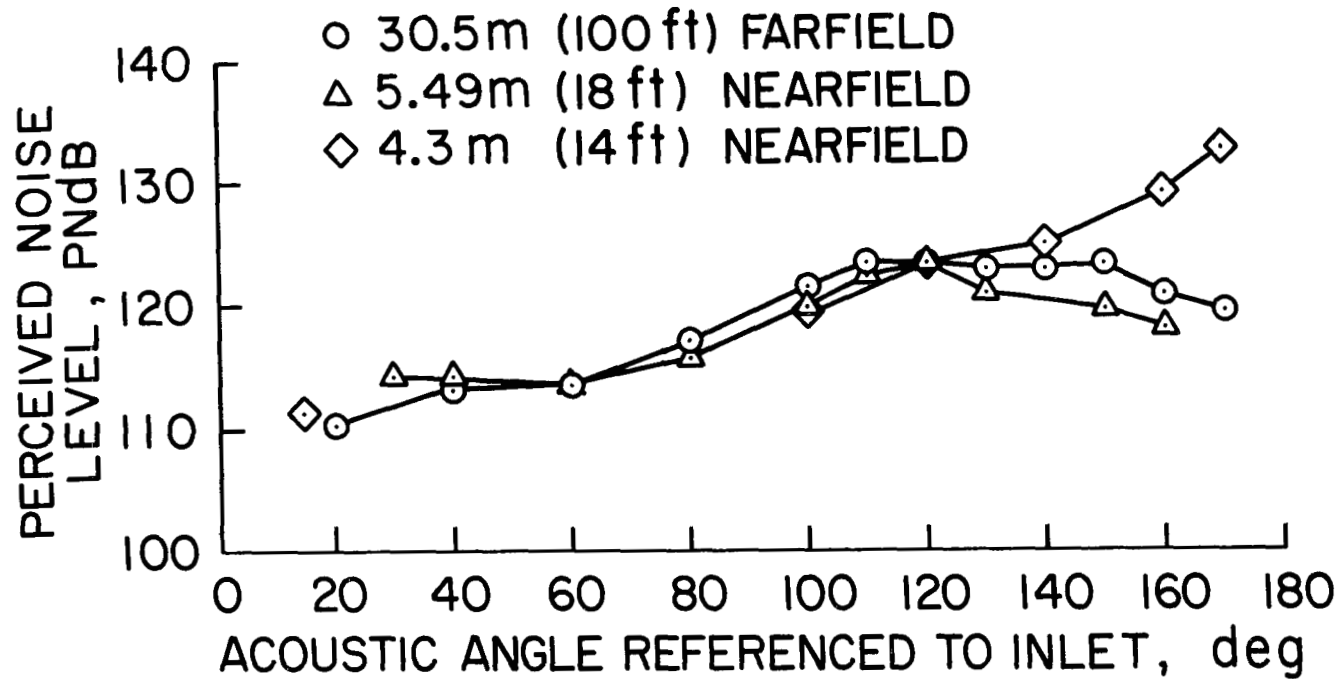


Figure 22.— Far-field to near-field comparison of PNL directivity for the 104-tube nozzle isolated nacelle installation, outdoor static test.

$\theta_I = 147^\circ$

$V_j = 518 \text{ m/sec (1700 ft/sec)}$

4.3 m (14 ft) SIDELINE

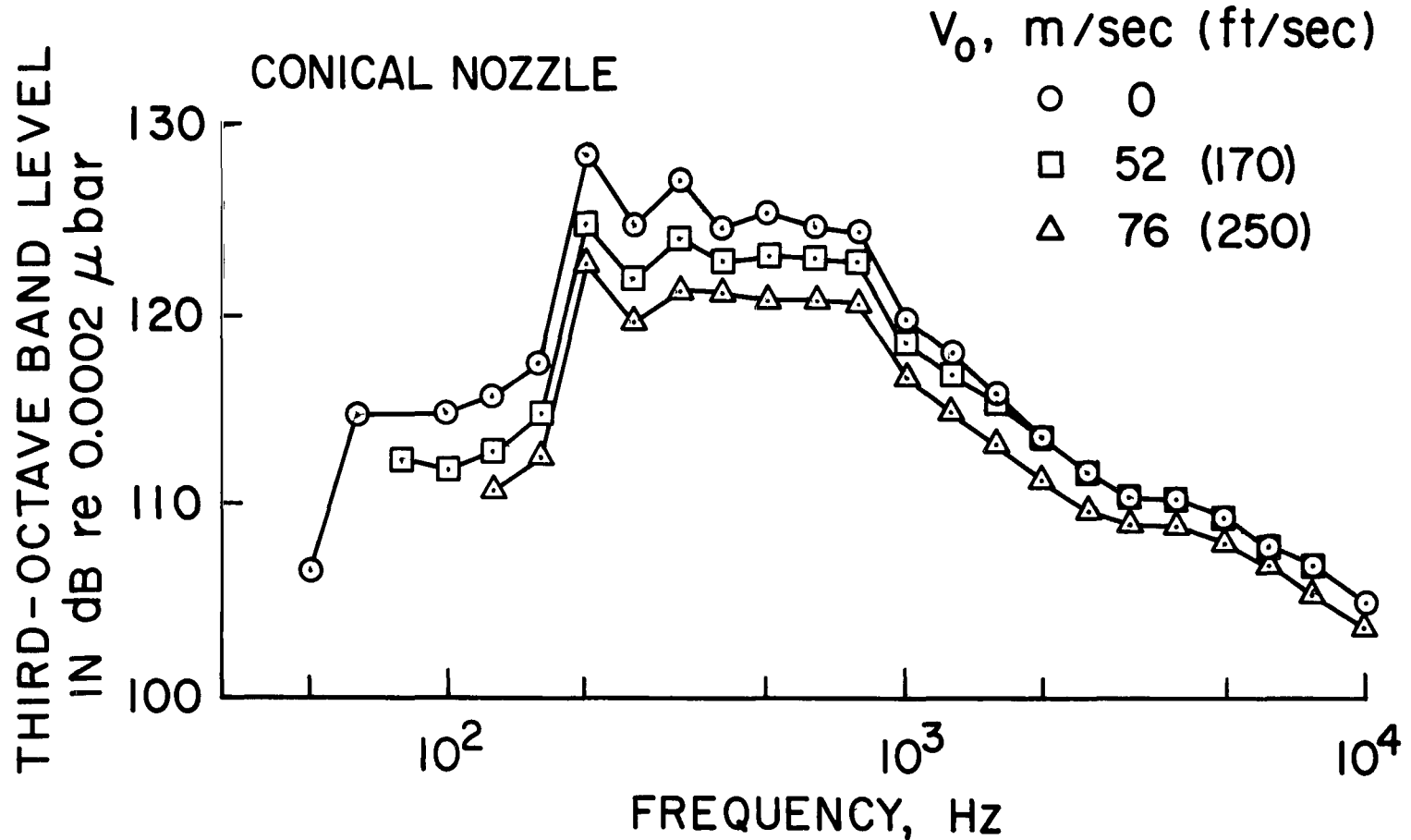


Figure 23.— 1/3-octave SPL spectrum conical ejector nozzle, wind-tunnel data, nacelle under wing installation.

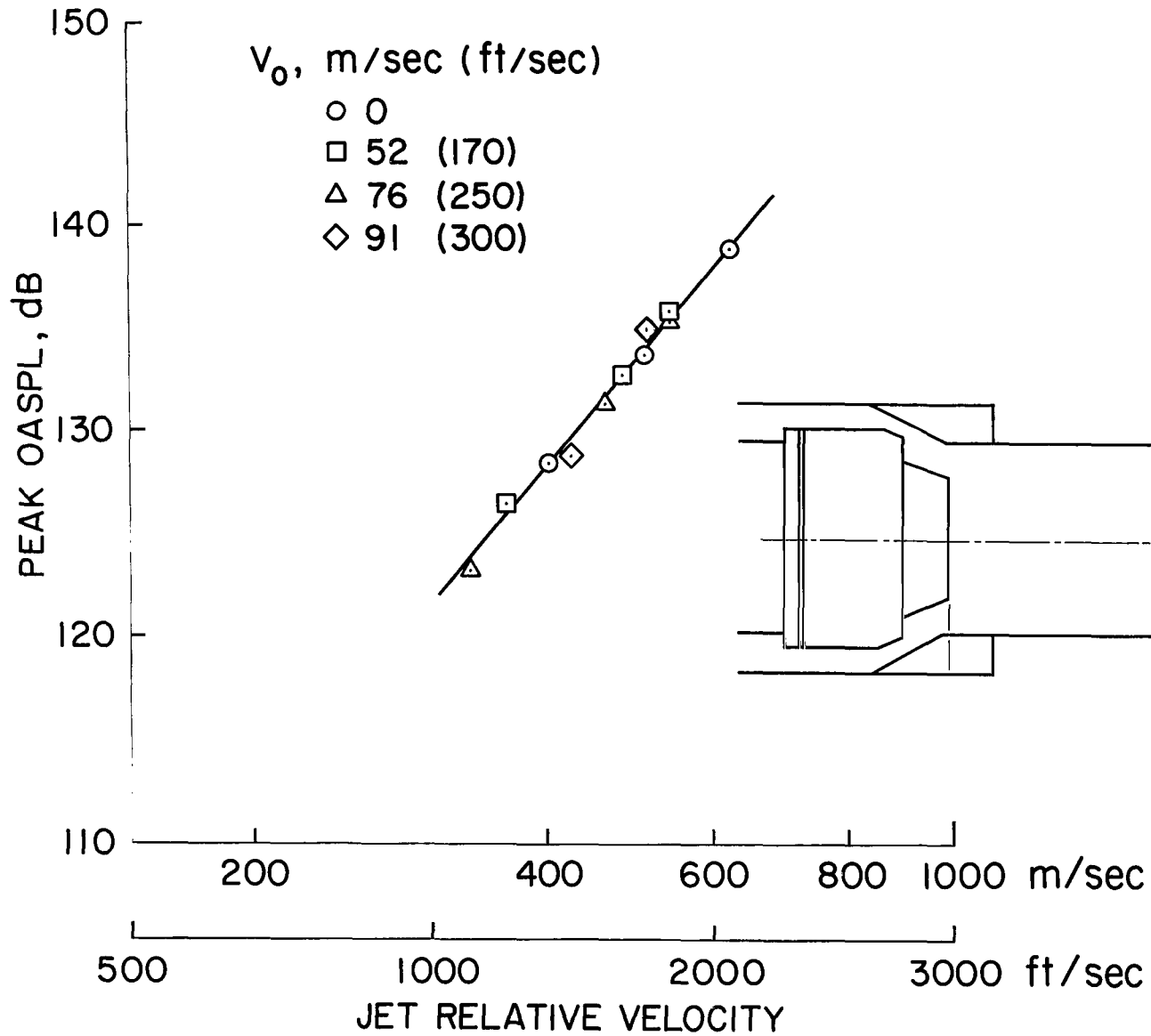


Figure 24.— Peak noise vs relative velocity for the conical nozzle, wind-tunnel data, nacelle under wing installation.

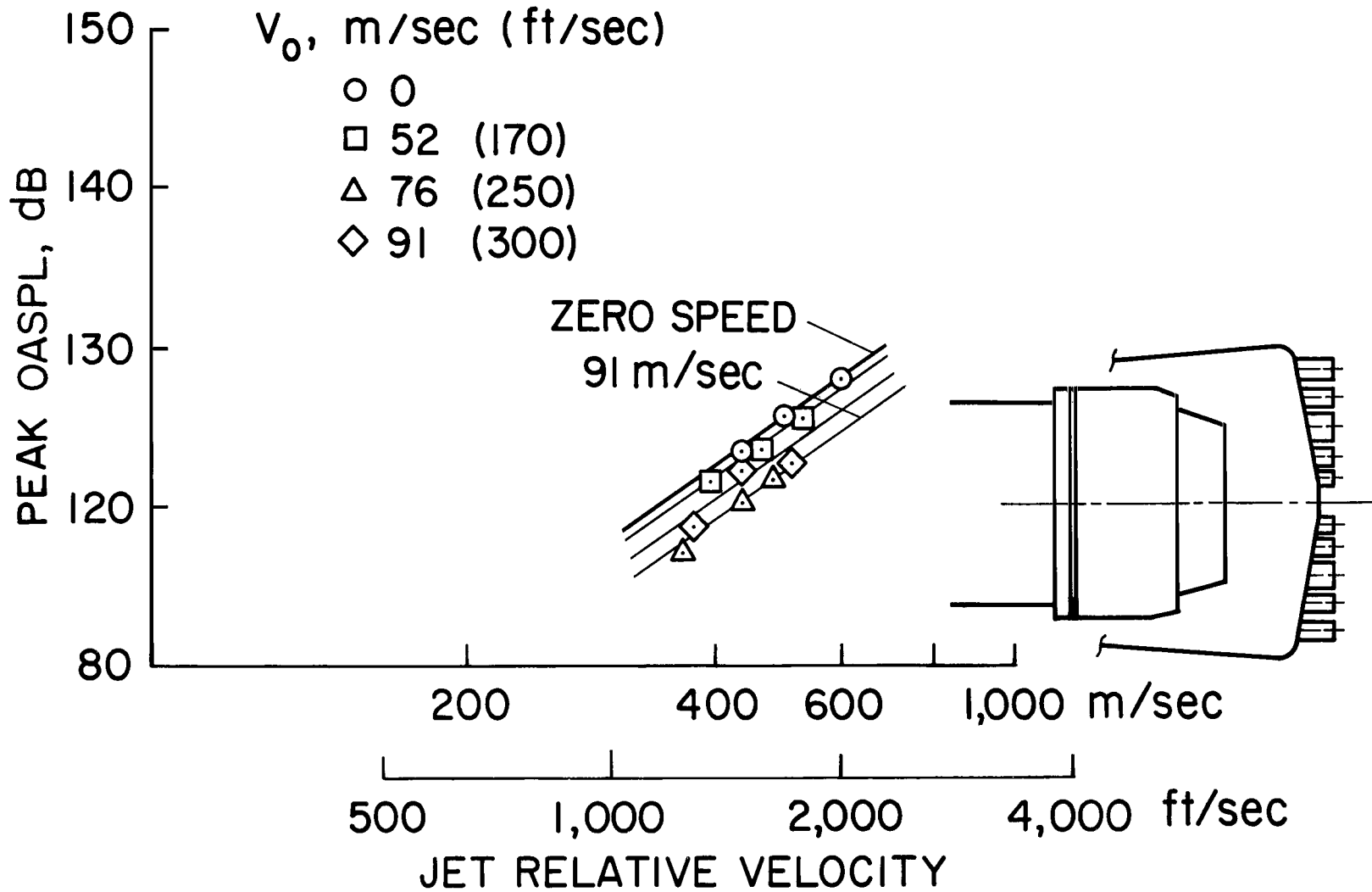


Figure 25.— Peak noise vs relative velocity for the 104-tube nozzle without acoustic shroud — wind-tunnel data, nacelle under wing installation.

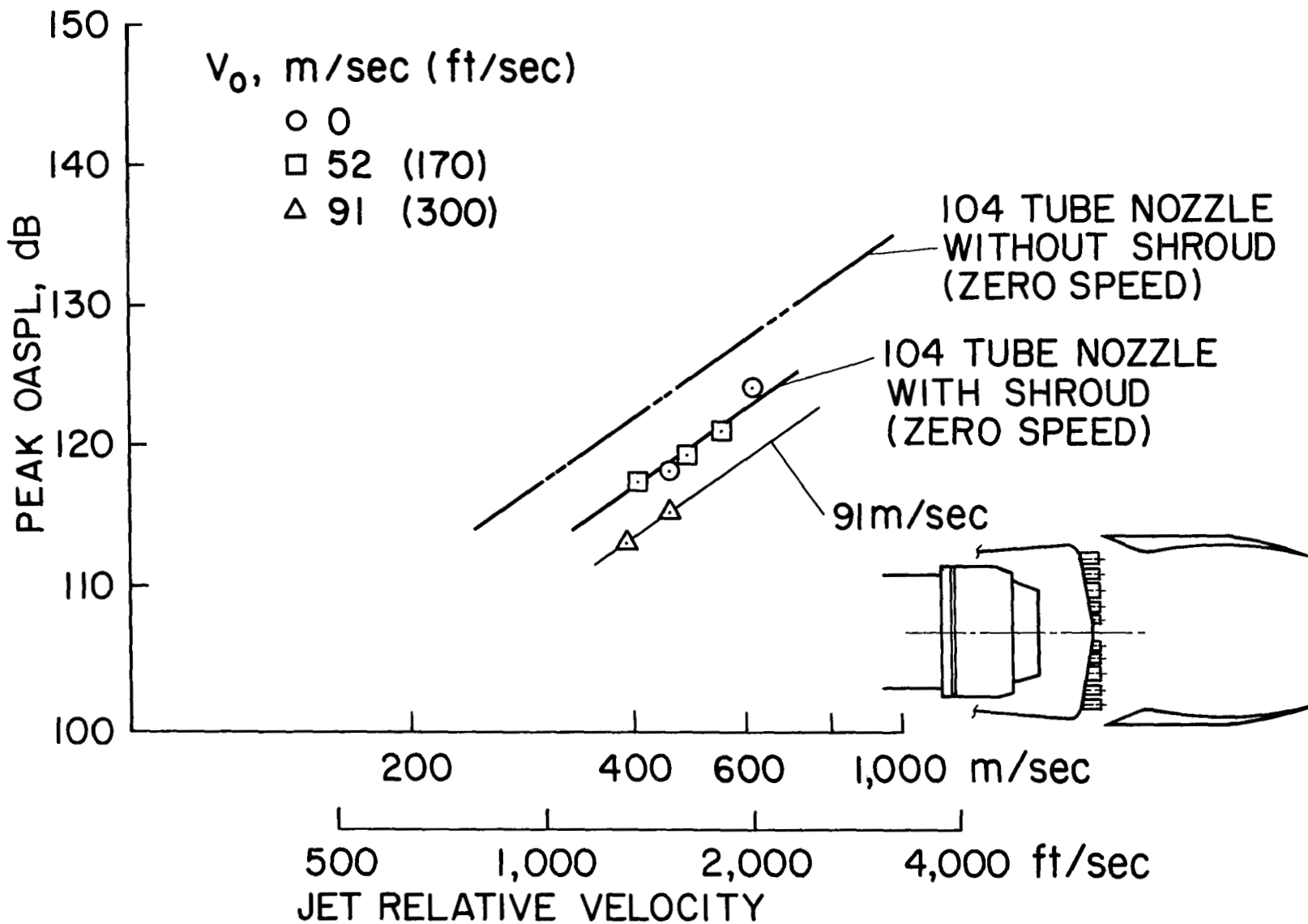


Figure 26.— Peak noise vs relative velocity for the 104-tube nozzle with the acoustic shroud — wind tunnel data, nacelle under wing installation.

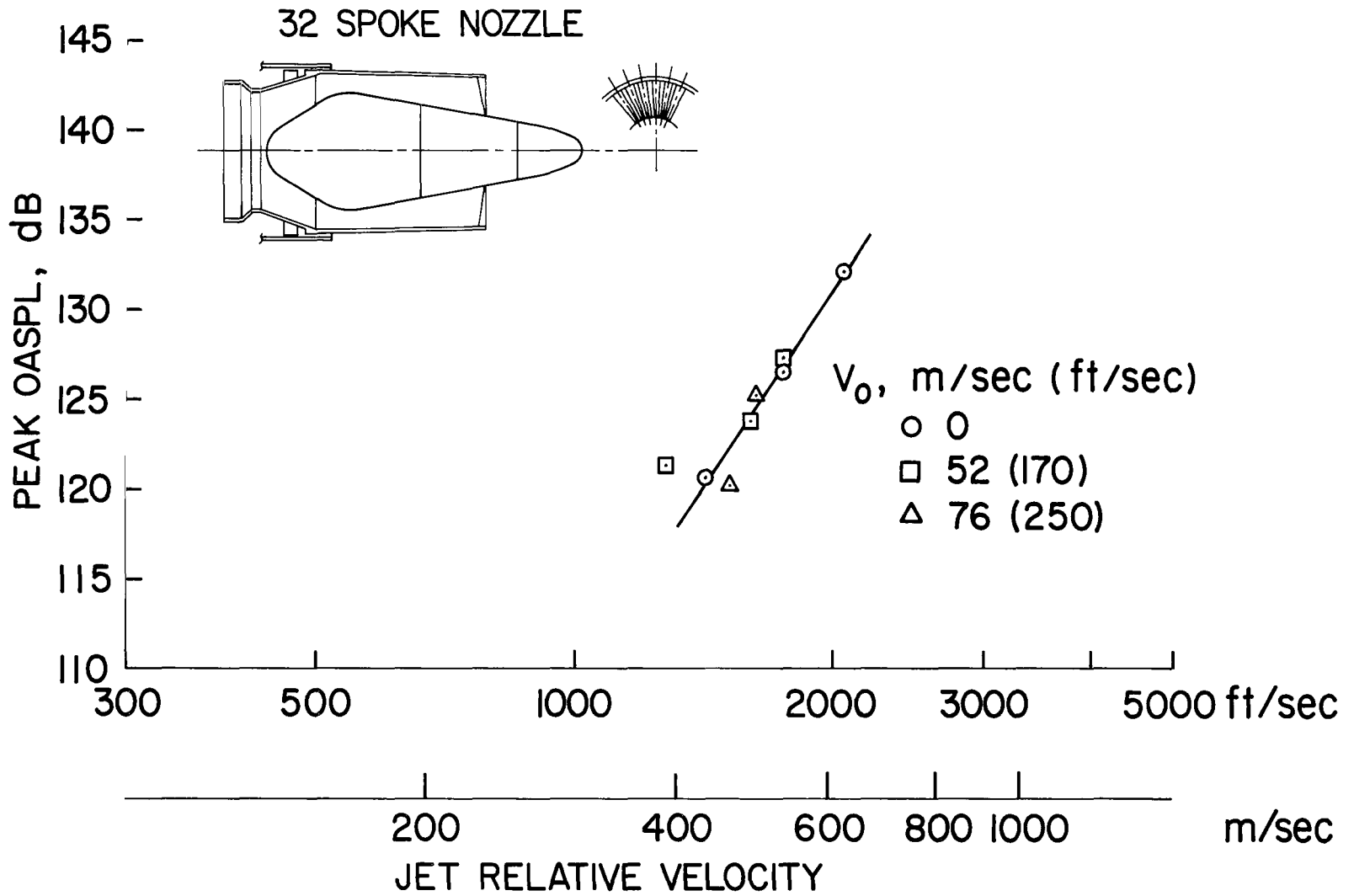


Figure 27.— Peak noise vs relative velocity for the 32-spoke nozzle, wind-tunnel data, nacelle under wing installation.

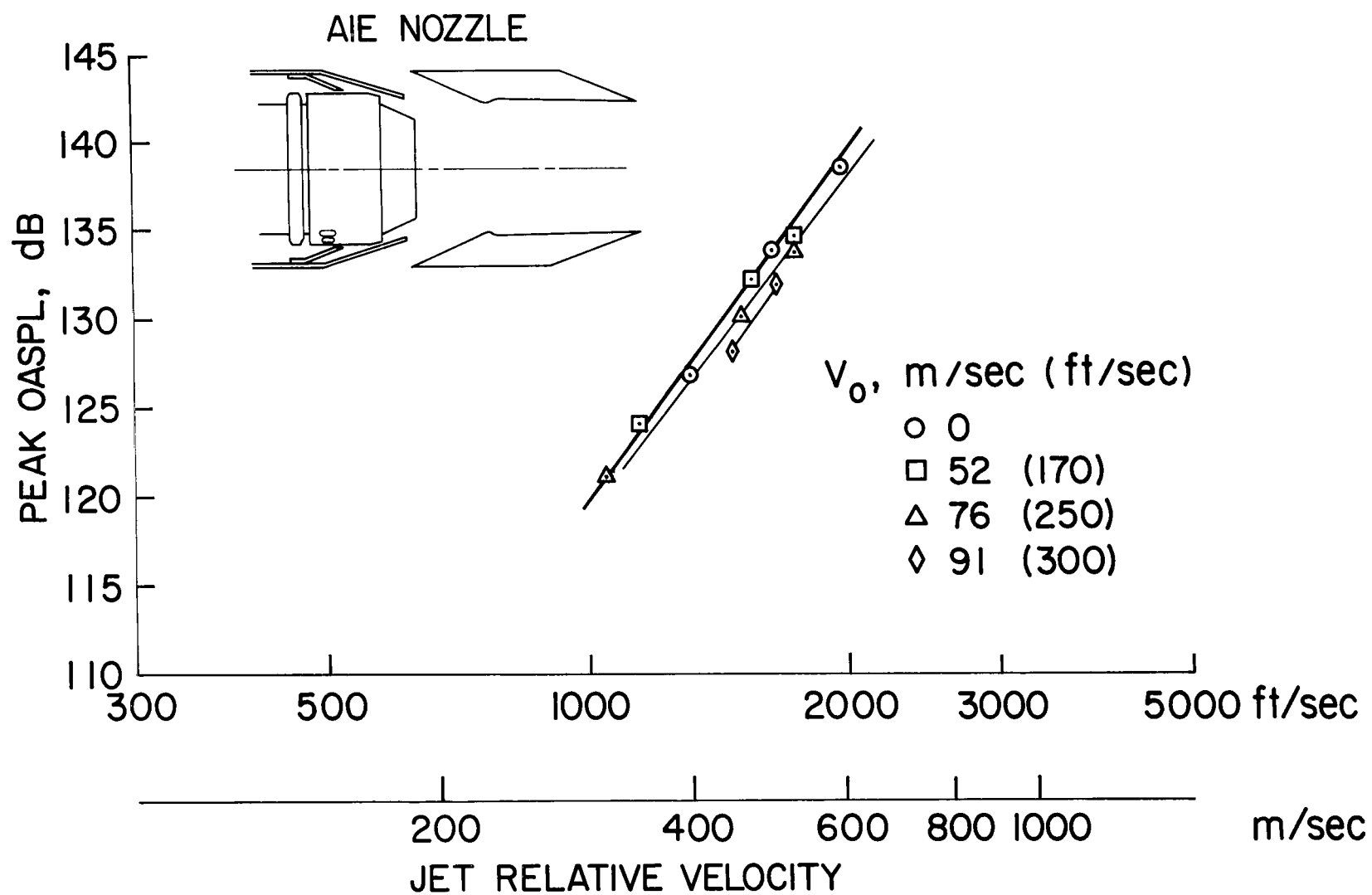


Figure 28.— Peak noise vs relative velocity for the AIE nozzle, wind-tunnel data, nacelle under wing installation.

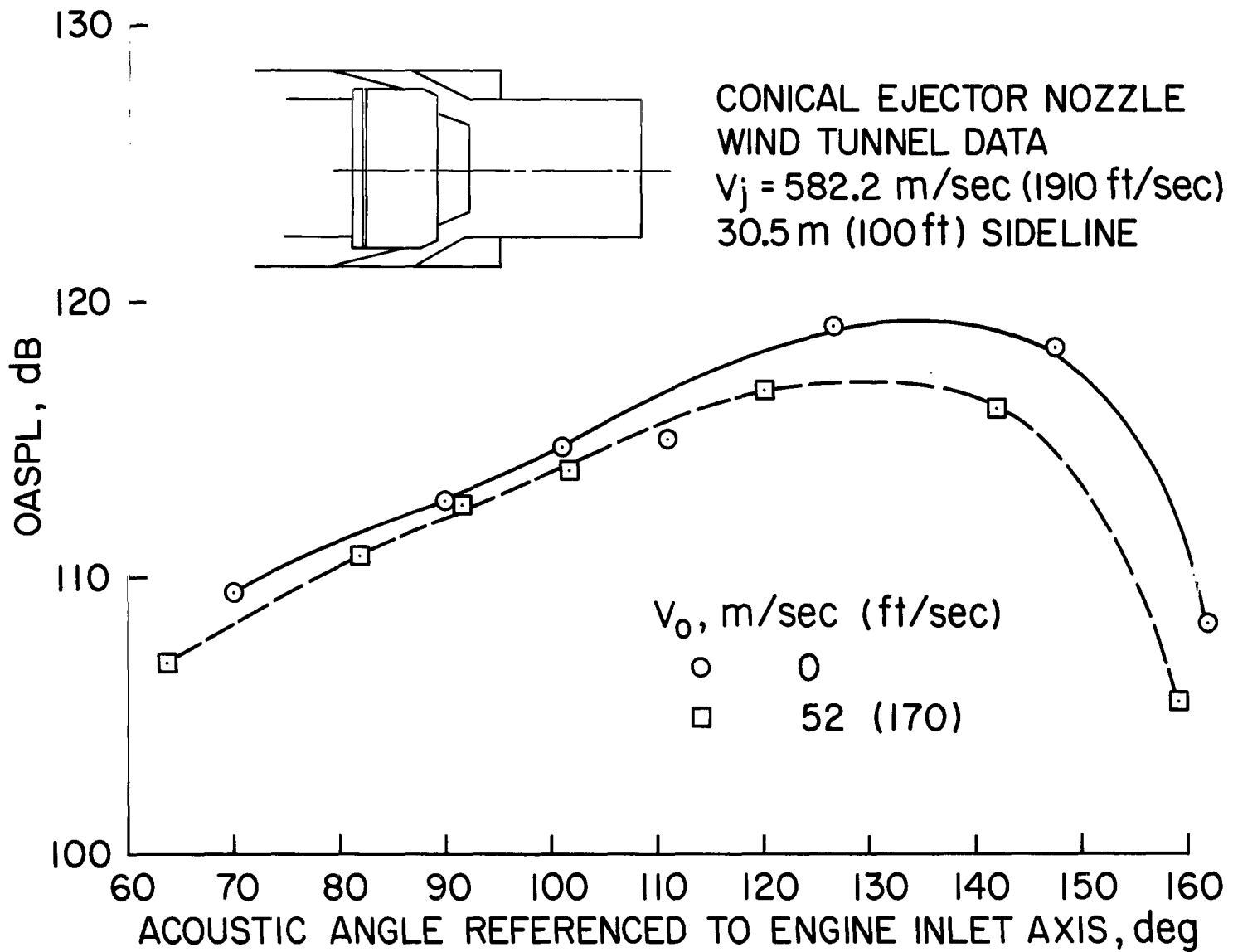


Figure 29.— OASPL directivity for conical ejector nozzle, wind-tunnel data, nacelle under wing installation, corrected for convection.

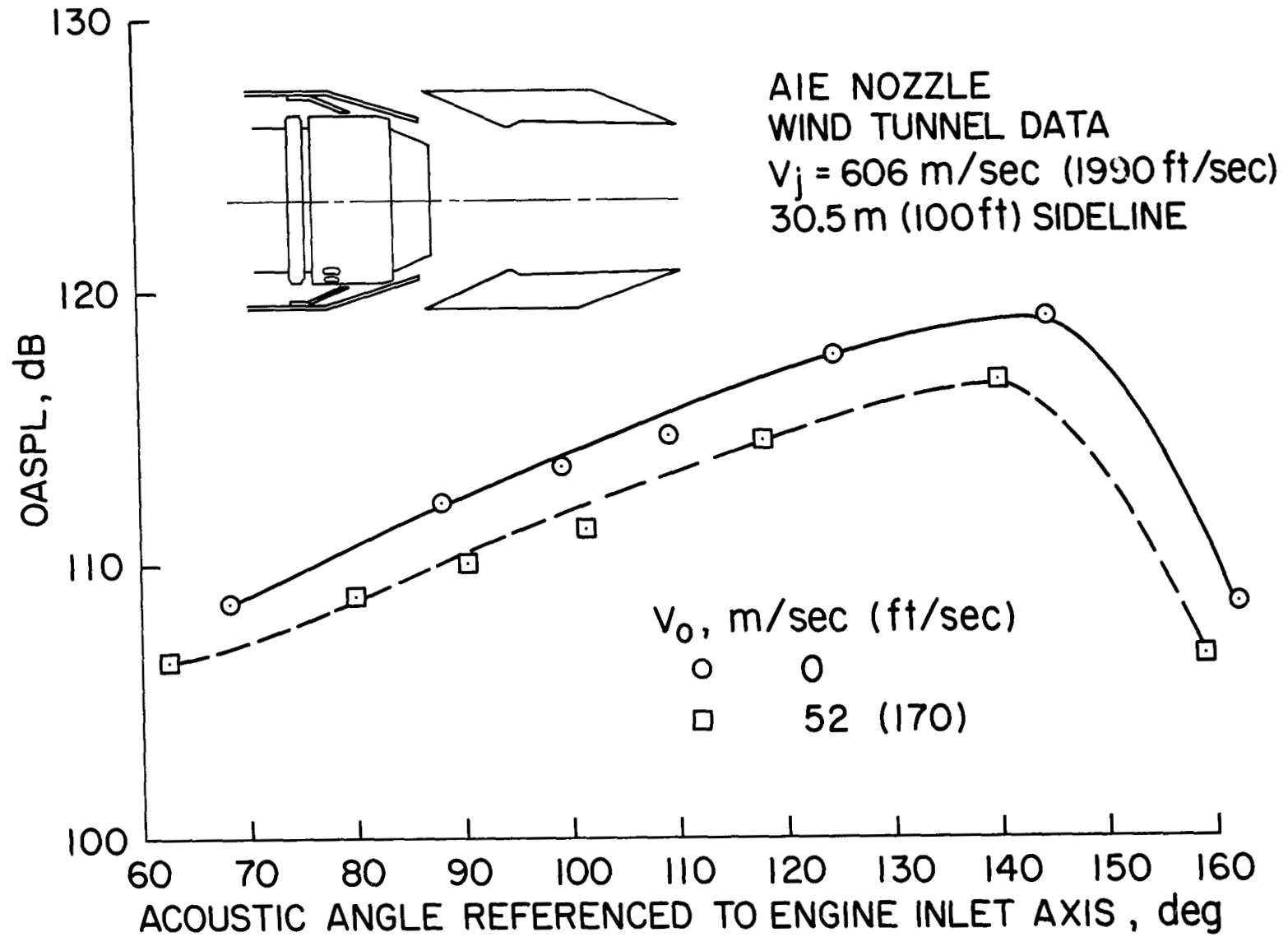


Figure 30.— OASPL directivity for AIE nozzle, wind-tunnel data, nacelle under wing installation, corrected for convection.

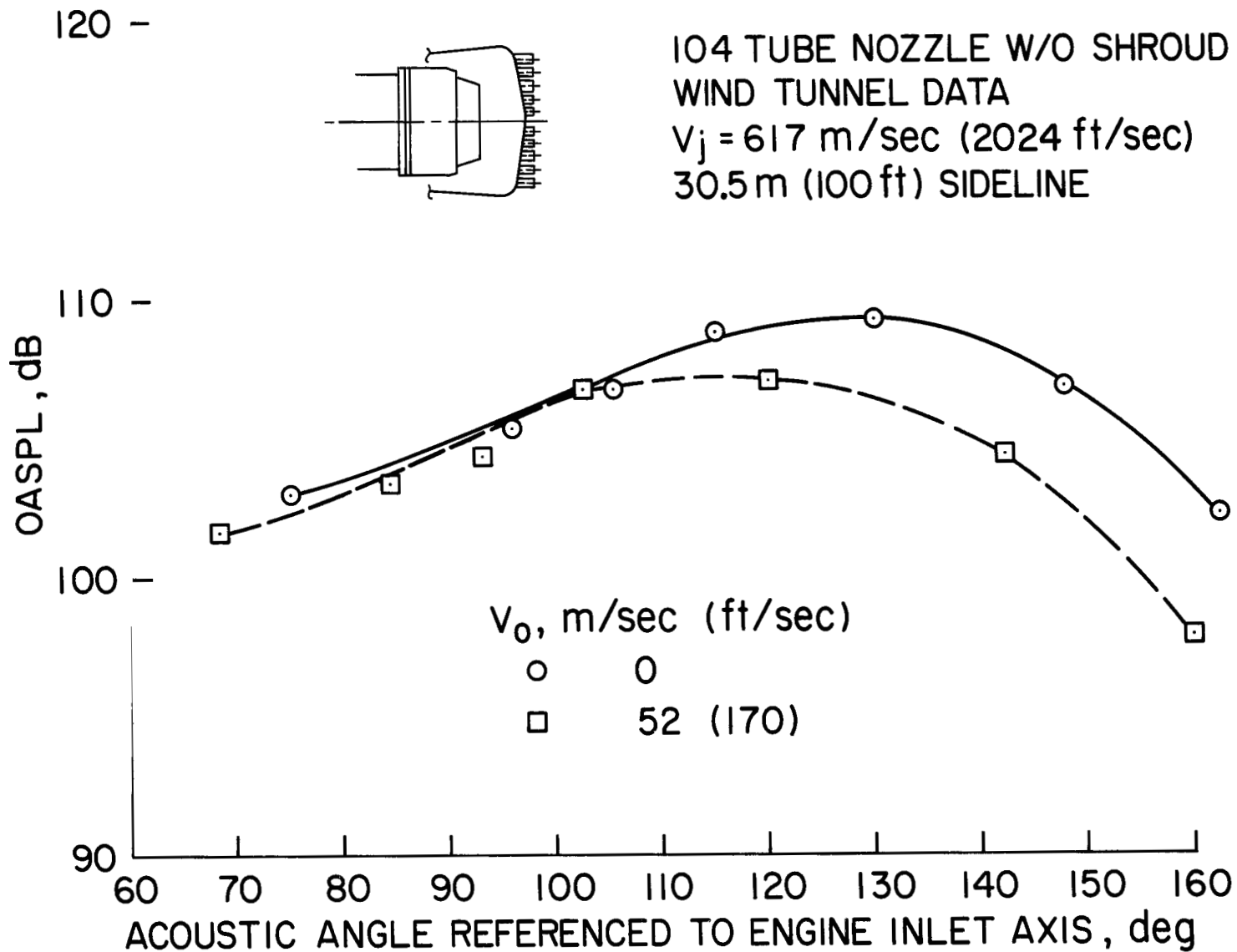


Figure 31.— OASPL directivity for 104-tube nozzle without shroud, wind-tunnel data, nacelle under wing installation, corrected for convection.

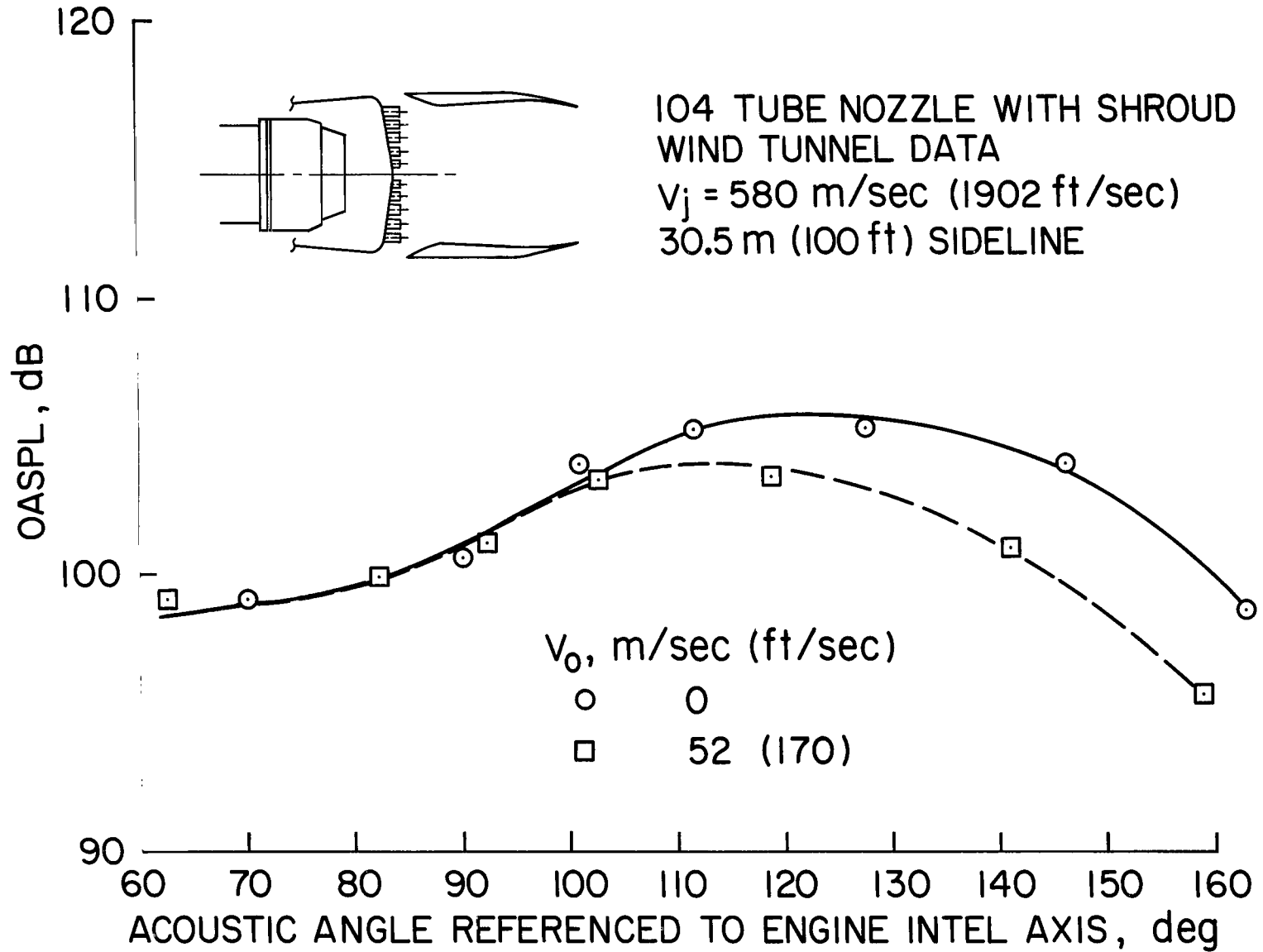


Figure 32.— OASPL directivity for 104-tube nozzle with acoustic shroud, wind-tunnel data, nacelle under wing installation, corrected for convection.

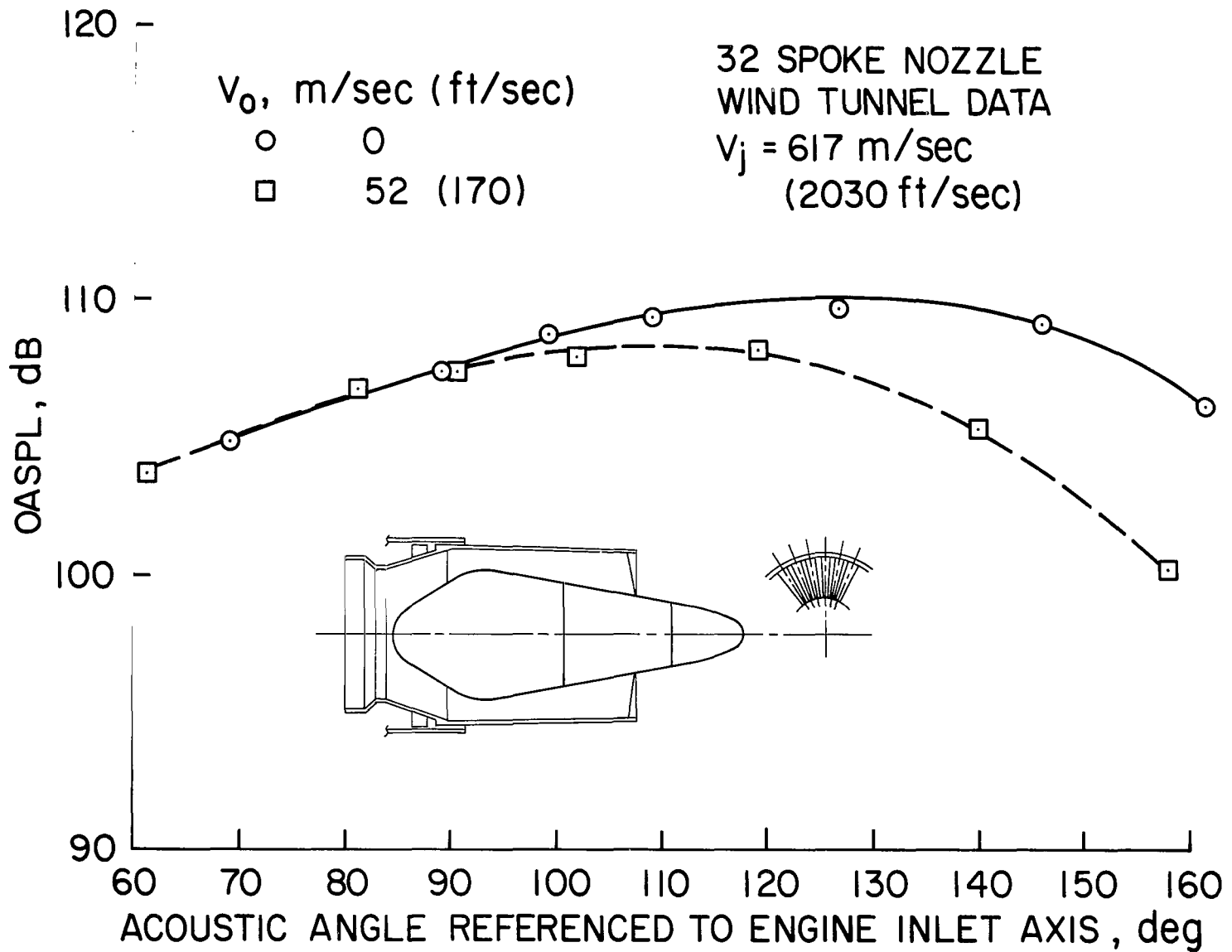


Figure 33.— OASPL directivity for 32-spoke nozzle, wind-tunnel data, nacelle under wing installation, corrected for convection.

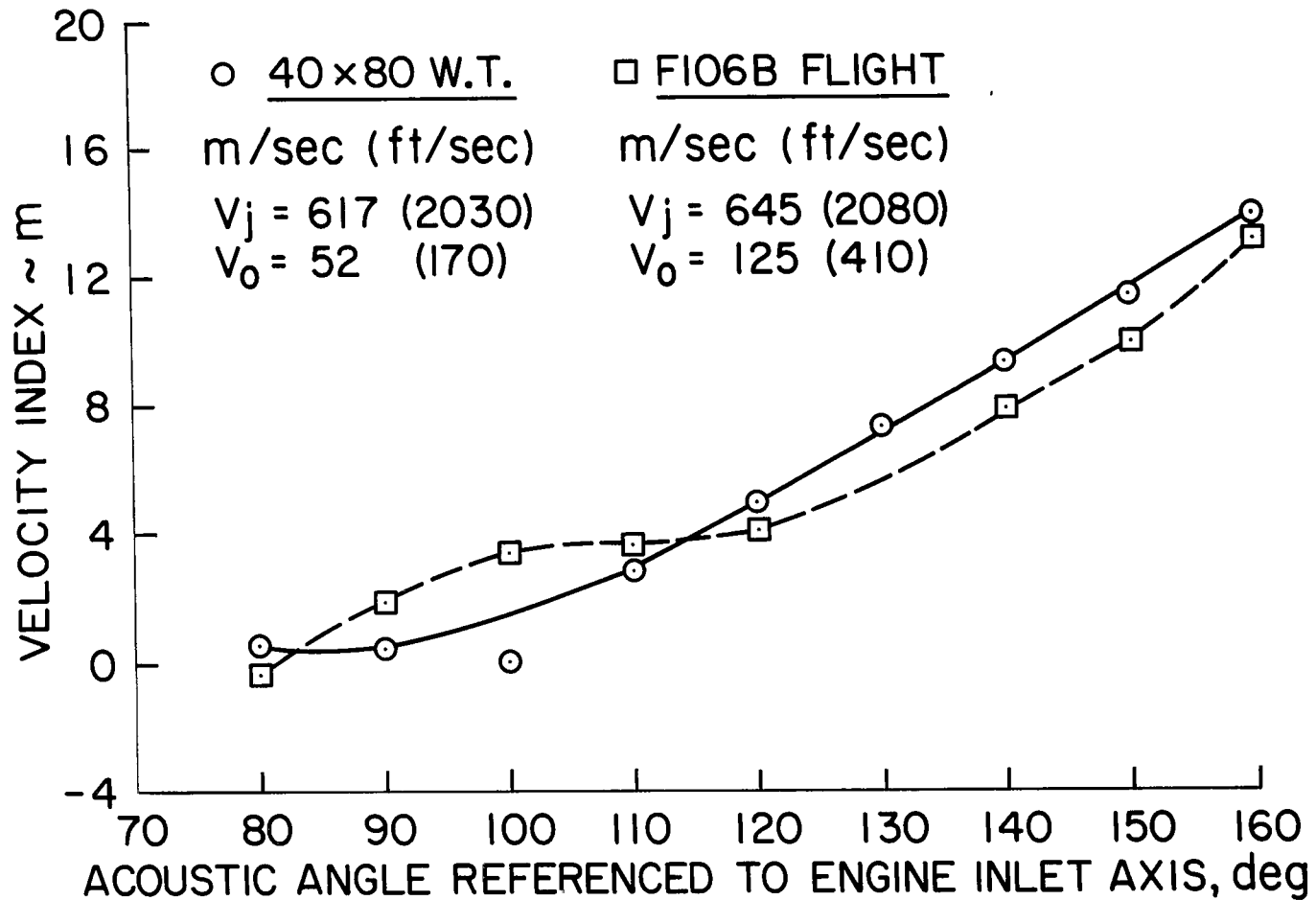


Figure 34.— Velocity index  $m$  vs acoustic angle from the engine inlet axis for the 104-tube nozzle without shroud; wind-tunnel data and F106B flight data.

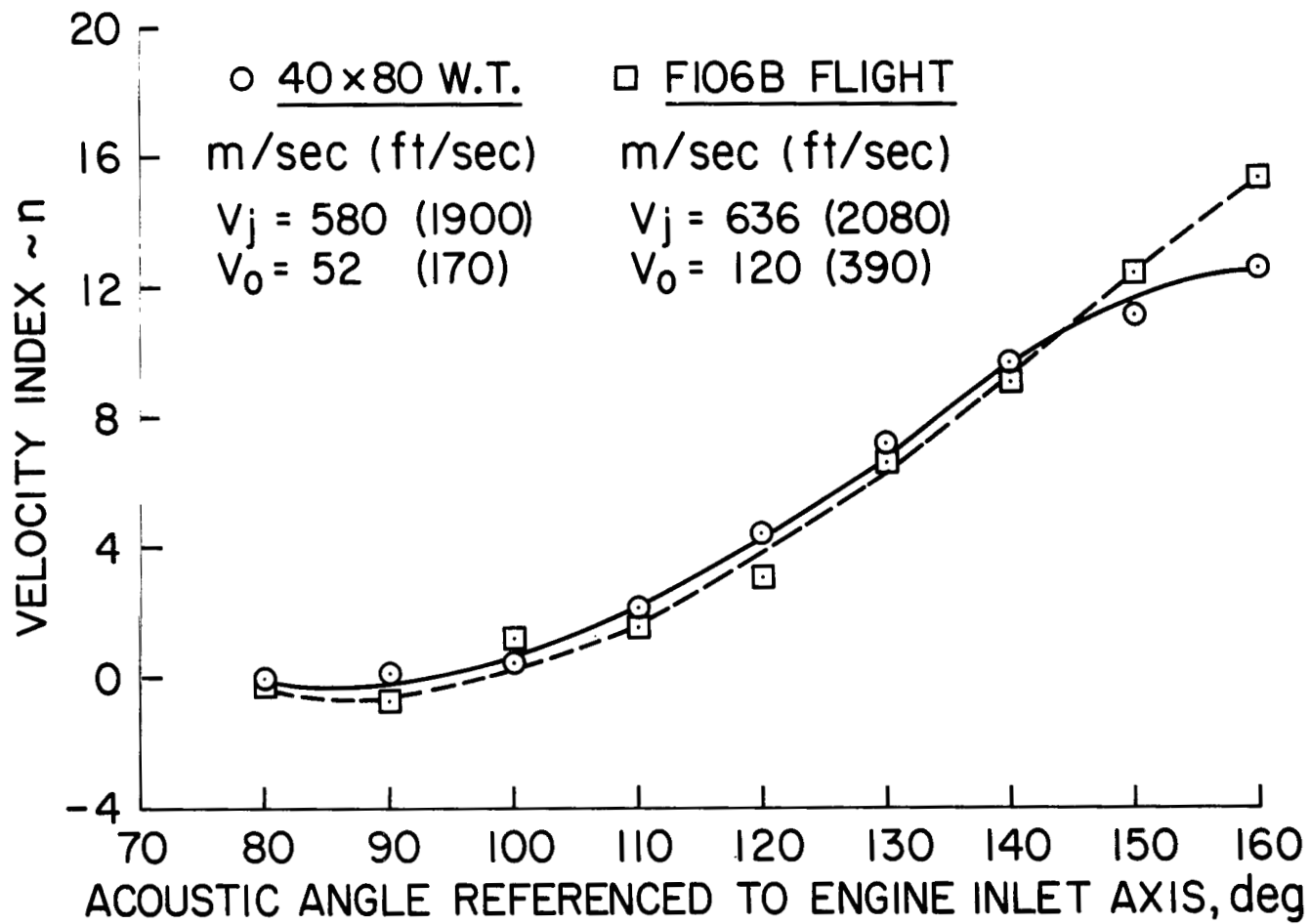


Figure 35.— Exponent  $m$  vs acoustic angle from the engine inlet axis for the 104-tube nozzle with acoustic shroud; wind-tunnel data and F106B flight data.

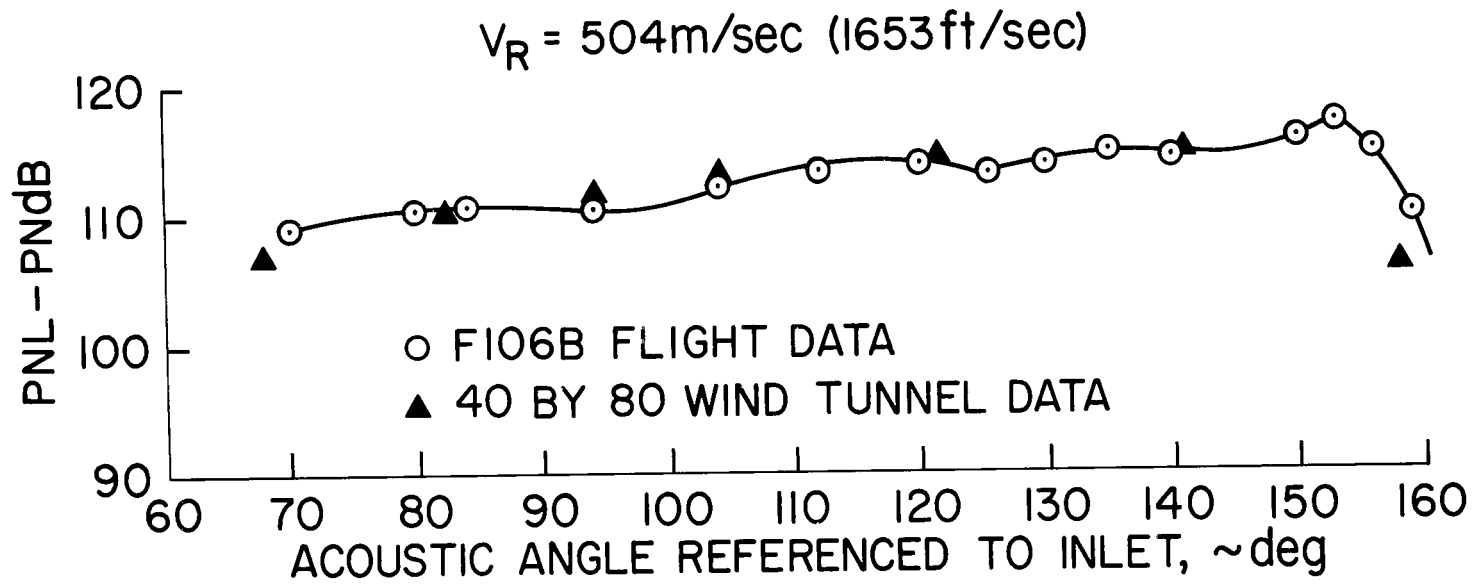


Figure 36.— Comparison of wind-tunnel data with flight data for the conical ejector nozzle; relative velocity of 504 m/sec (1653 ft/sec) PNL directivity.

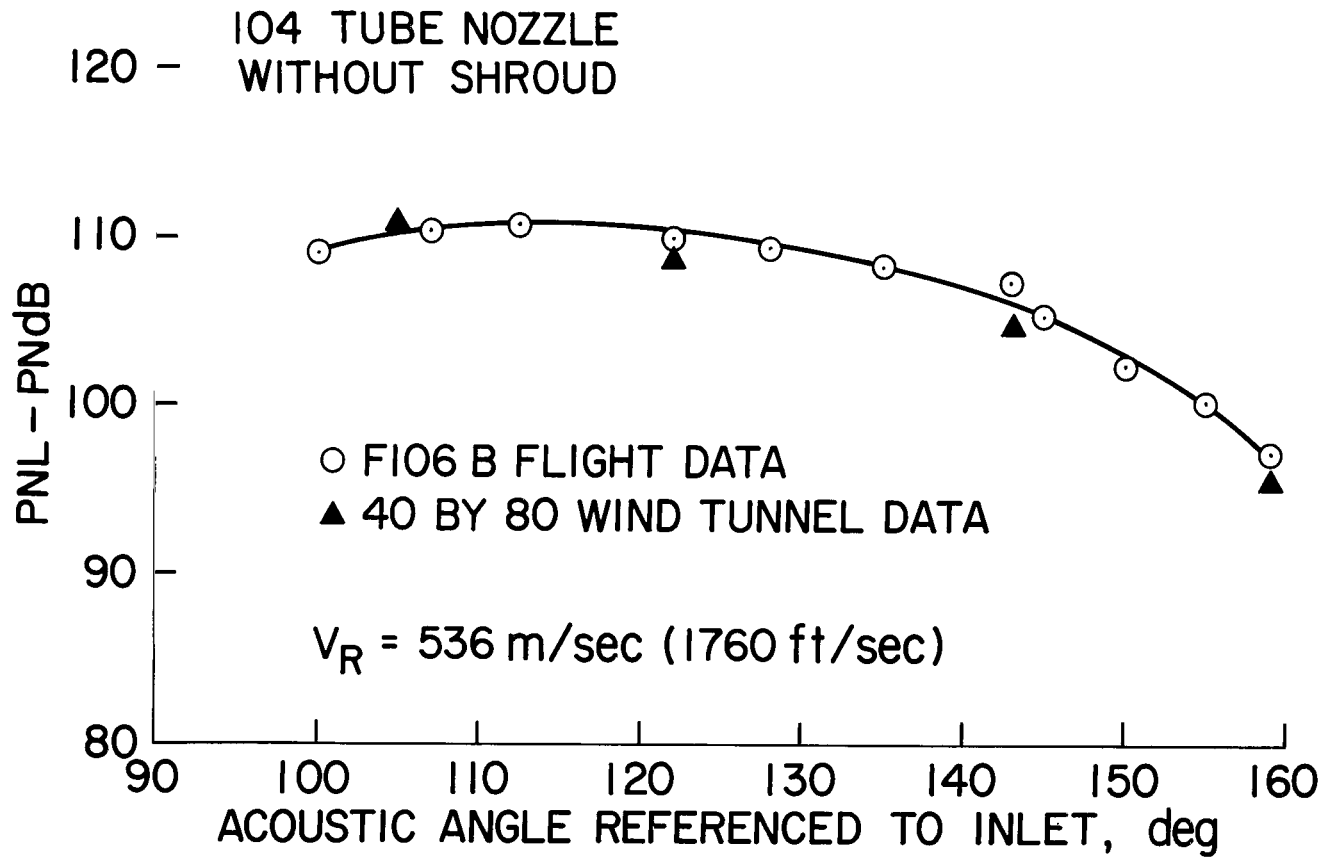


Figure 37.— Comparison of wind-tunnel data with flight data for the 104-tube nozzle without shroud; relative velocity, 536 m/sec (1760 ft/sec) PNL directivity.

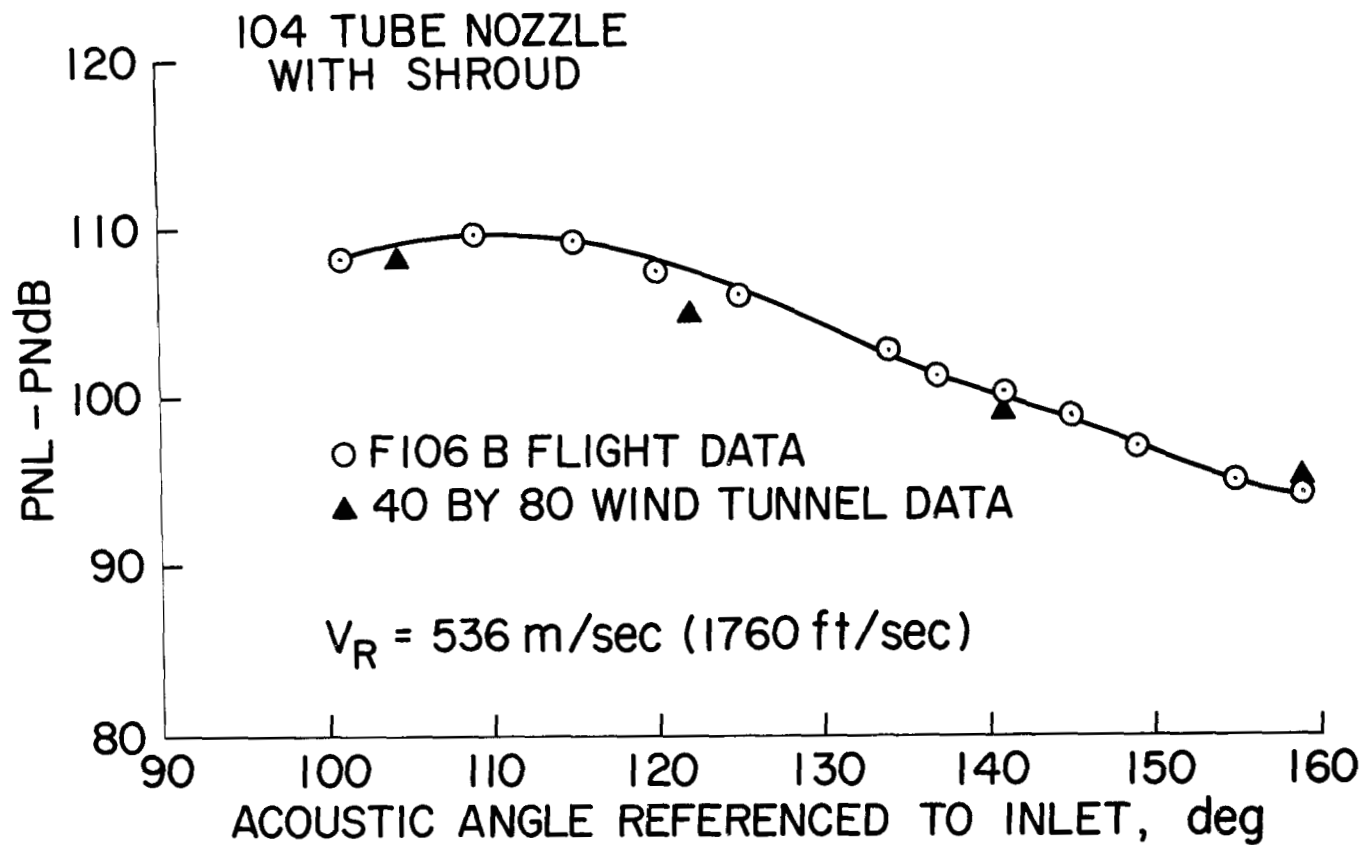


Figure 38.— Comparison of wind-tunnel data with flight data for the 104-tube nozzle with shroud; relative velocity, 536 m/sec (1760 ft/sec) PNL directivity.

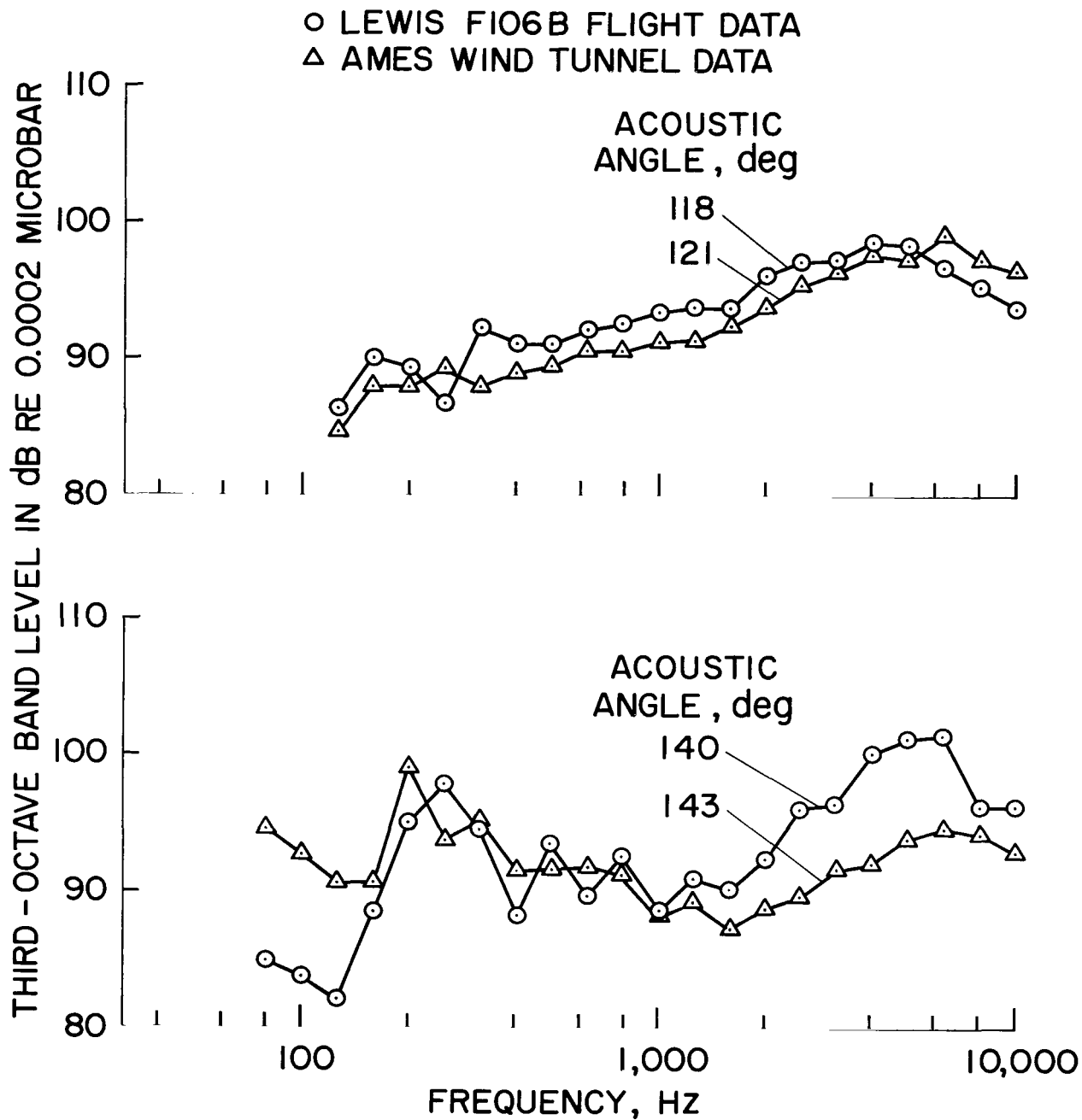


Figure 39.— Comparison of 1/3-octave SPL spectrums from wind tunnel and flight data for the 104 elliptical tube nozzle without acoustic shroud; relative velocity, 536 m/sec (1760 ft/sec).



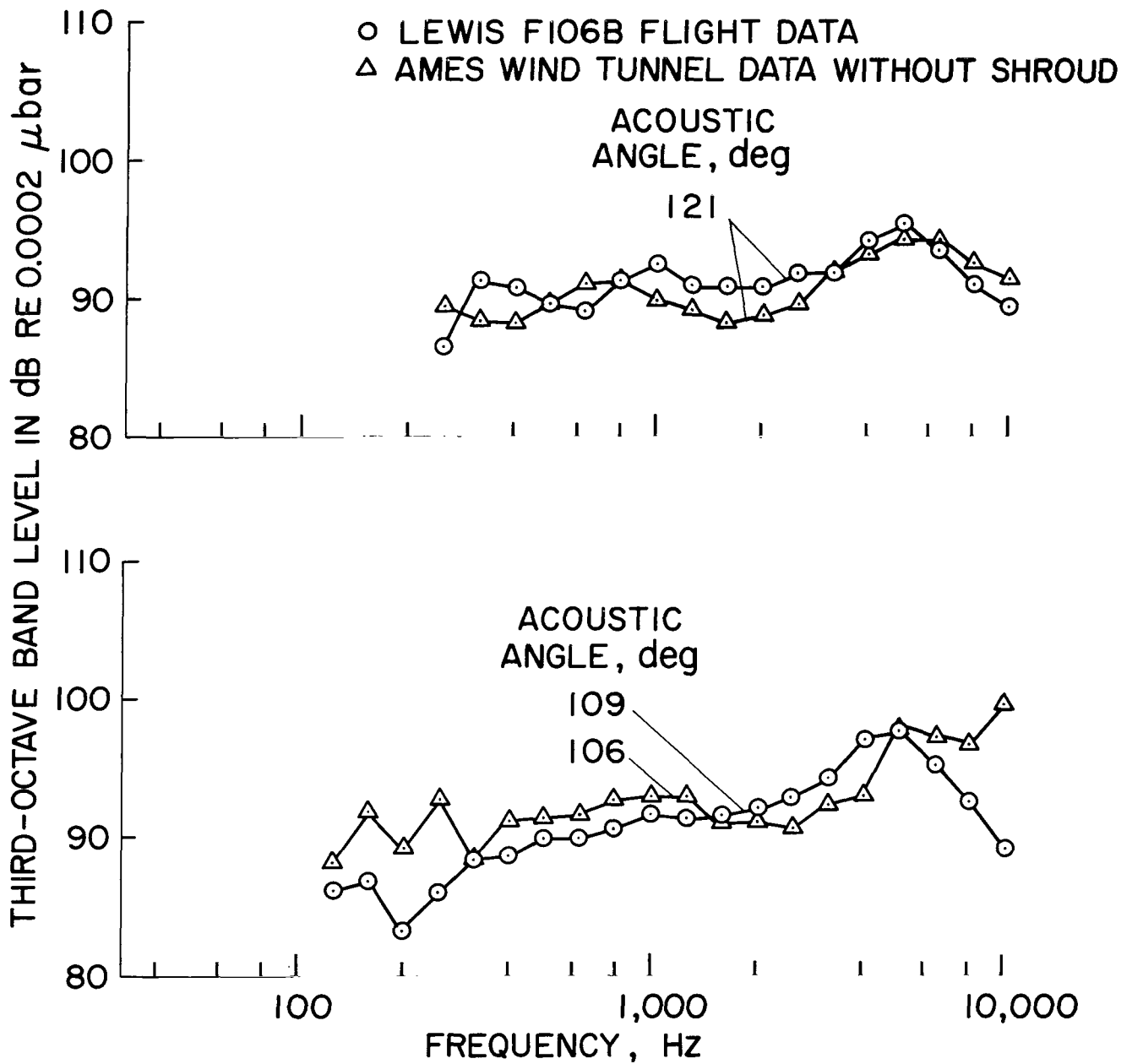


Figure 40.— Comparison of 1/3-octave SPL spectrums from wind tunnel and flight data for the 104-tube nozzle with the acoustic shroud; relative velocity, 536 m/sec (1760 ft/sec).

NATIONAL AERONAUTICS AND SPACE ADMINISTRATION  
WASHINGTON, D.C. 20546

OFFICIAL BUSINESS  
PENALTY FOR PRIVATE USE \$300

SPECIAL FOURTH-CLASS RATE  
BOOK

POSTAGE AND FEES PAID  
NATIONAL AERONAUTICS AND  
SPACE ADMINISTRATION  
451



083 001 C1 U A 770128 S00903DS  
DEPT OF THE AIR FORCE  
AF WEAPONS LABORATORY  
ATTN: TECHNICAL LIBRARY (SUL)  
KIRTLAND AFB NM 87117

POSTMASTER: If Undeliverable (Section 158  
Postal Manual) Do Not Return

*"The aeronautical and space activities of the United States shall be conducted so as to contribute . . . to the expansion of human knowledge of phenomena in the atmosphere and space. The Administration shall provide for the widest practicable and appropriate dissemination of information concerning its activities and the results thereof."*

—NATIONAL AERONAUTICS AND SPACE ACT OF 1958

## NASA SCIENTIFIC AND TECHNICAL PUBLICATIONS

**TECHNICAL REPORTS:** Scientific and technical information considered important, complete, and a lasting contribution to existing knowledge.

**TECHNICAL NOTES:** Information less broad in scope but nevertheless of importance as a contribution to existing knowledge.

**TECHNICAL MEMORANDUMS:** Information receiving limited distribution because of preliminary data, security classification, or other reasons. Also includes conference proceedings with either limited or unlimited distribution.

**CONTRACTOR REPORTS:** Scientific and technical information generated under a NASA contract or grant and considered an important contribution to existing knowledge.

**TECHNICAL TRANSLATIONS:** Information published in a foreign language considered to merit NASA distribution in English.

**SPECIAL PUBLICATIONS:** Information derived from or of value to NASA activities. Publications include final reports of major projects, monographs, data compilations, handbooks, sourcebooks, and special bibliographies.

**TECHNOLOGY UTILIZATION PUBLICATIONS:** Information on technology used by NASA that may be of particular interest in commercial and other non-aerospace applications. Publications include Tech Briefs, Technology Utilization Reports and Technology Surveys.

*Details on the availability of these publications may be obtained from:*

**SCIENTIFIC AND TECHNICAL INFORMATION OFFICE**

**NATIONAL AERONAUTICS AND SPACE ADMINISTRATION**  
Washington, D.C. 20546